UNIVERSITA' DEGLI STUDI DI MESSINA

DIPARTIMENTO DI MEDICINA CLINICA E SPERIMENTALE

XXIX CICLO DI DOTTORATO IN
SCIENZE BIOMEDICHE CLINICHE E SPERIMENTALI

THERAPEUTIC ANGIOGENESIS IN DIABETES-RELATED IMPAIRED WOUND HEALING

TESI DI DOTTORATO:
Dott. Carmelo Gabriele PIZZINO

RELATORE:
Ch.mo Prof. Francesco Squadrito

CO-RELATORE:
Prof.ssa Alessandra Bitto

ANNO ACCADEMICO 2015/2016

TABLE OF CONTENTS

Introduction

Diabetic ulcers

Patients suffering from diabetes show a disturbed wound healing process that may enhance the overall morbidity and mortality of this population [Falanga, 2005; Singh et al., 2005].

The main underlying risk factors for foot ulceration are peripheral neuropathy and ischaemia. These changes can lead to pure neuropathic ulcers, pure ischaemic ulcers or mixed neuroischaemic ulcers. Symmetrical distal polyneuropathy encompasses motor, sensory and autonomic nerves. This leads to changes in the structure of the foot that increase pressure loading. The loss of painful stimulus allows the patient inadvertently to injure the foot either suddenly or gradually. Loss of sweating may lead to dry and cracked skin, and changes in local microvascular circulation predispose to infection and poor oxygenation of tissues. Atherosclerosis is 20 times more common in the lower limbs of diabetic patients, usually affecting the distal main vessels, but often sparing the pedal vessels. The resultant ischaemia not only causes ulceration; it also hinders wound healing, turning a wound into a chronic ulcer. The initial rate of tissue repair is significantly related to local cutaneous perfusion, estimated by peri-wound partial pressure of oxygen and carbon dioxide; eventual ulcer re-epithelialization is also related to absolute foot blood pressure.

Once a wound has developed, current best practice involves wound assessment and classification into ischaemic, neuropathic or neuroischaemic ulcer types, offloading of pressure on the area, frequent debridement, dressings and management of infection. More aggressive surgical treatment may be indicated for ulcers or infections that do not improve with good non-surgical treatment. Resection of infected bone may be part of a wider debridement back to healthy tissue. Vascular reconstruction is indicated in limbs with inadequate peripheral perfusion. This may involve angioplasty or surgical bypass. Amputation may ultimately be necessary in patients with non-reconstructable vascular disease or extensive osteomyelitis. This may be a minor resection of a toe or forefoot if the peripheral circulation is sufficient to allow healing of the subsequent wound, but a major amputation may be required at below- or above-knee level. Recent introductions aimed at promoting wound healing include hyperbaric oxygen therapy and artificial skin grafting. In spite of these interventions, a cohort of patients with foot ulcers remains unresponsive to available conventional treatment, thus new treatments are needed.

The healing process

A complex programmed sequence of cellular and molecular processes including inflammation, cell migration, angiogenesis, provisional matrix

synthesis, collagen deposition and re-epithelization characterizes the normal skin repair [Falanga, 2005; Reiber and Raugi, 2005]. Wound healing proceeds through a series of consecutive, but overlapping, stages, characterized by the sequential movement of different cell populations into the wound site. In broad outline, this involves: the formation of a blood clot and fibrin-based provisional matrix; the ingress of neutrophils and monocytes; the initiation of epithelial cell migration; the growth of new blood vessels from pre-existing ones (angiogenesis); the coordinate migration of fibroblasts and new blood vessels into the wound site to produce granulation tissue; re-epithelialization of the wound surface; collagen deposition by granulation tissue fibroblasts and matrix remodelling; and the formation of a relatively acellular mature scar consisting predominantly of type I collagen bundles.

At the molecular level, the acute wound healing response is characterized by changes in the composition and organization of the extracellular matrix and local profile of growth factors. In response to these regulatory molecules, infiltrating leucocytes and resident tissue cells (keratinoyctes, fibroblasts and endothelial cells) undergo sequential alterations in cell morphology, proliferation, migratory activity and gene expression, which collectively define the process of cell activation. The complementary processes of cell deactivation, return to the resting phenotype, and apoptosis of the remaining

activated cells mark the end of the wound healing response. The wound gains about 20 per cent of its final strength in the first 3 weeks of healing, but further gain in strength takes longer. The final scar regains about 70 per cent of the strength of intact skin.

Healing impairment in diabetic patients is characterized by delayed cellular infiltration and granulation tissue formation, decreased collagen organization and, more interestingly, reduced angiogenesis [Ferrara et al., 2003, Tammela et al., 2005].

Angiogenesis and Vasculogenesis

Angiogenesis plays a central role in wound healing and is associated with expression of several cytokines, and angiogenic factors, such as vascular endothelial growth factor (VEGF) [Ferrara et al., 2003, Tammela et al., 2005].

As far as angiogenesis is concerned a defect in VEGF regulation, characterized by an altered expression pattern of VEGF mRNA during skin repair, has been shown in diabetic mice [Altavilla et al., 2001]. In addition, it has been reported that adeno-associated viral vector (AAV)-mediated human VEGF165 gene transfer, stimulates angiogenesis and wound healing in the genetically diabetic mice [Galeano et al., 2003].

Besides angiogenesis, vasculogenesis may also play a crucial role in the healing process. Vasculogenesis, the in situ differentiation of the primitive endothelial progenitors known as angioblasts into endothelial cells that aggregate into a primary capillary plexus, has been shown to be responsible for the development of the vascular system during embryogenesis [Peichev et al., 2000]. However, vasculogenesis is also present in adults and occurs through the action of circulating or resident bone marrow-derived cells called endothelial progenitor cells (EPCs), and may be also primed by VEGF [Asahara et al., 1999]. Further cell-lineages not bone-marrow derived may be found at different sites and have been demonstrated to differentiate into endothelial cells under hypoxic conditions or during physiologic replenishment of skin and gut [Urbich et al., 2004]. Moreover vasculogenesis is more prevalent and effective when angiogenesis is failing: this is the case of the healing of diabetic ulcers in which there is an impairment of haemostasis, inflammation, matrix deposition and most of all angiogenesis [Wetzler et al., 2000]. EC progenitors circulating and wound–level numbers are also decreased in diabetes, implicating an abnormality in EC progenitors mobilization and homing mechanisms [Brem et al., 2007]. The deficiency in EC progenitors mobilization is presumably due to the impairment in the eNOS-NO cascade in the bone marrow (BM) and the EC progenitors failure to reach to the wound tissues is partly a result of a down-regulated production

of stromal cell-derived factor 1α (SDF-1α) in the wounds [Brem et al., 2007]. In fact SDF-1α, by binding to its receptor CXCR4 on EC progenitors, allows the recruitment and homing of these cells in hypoxic tissues [Brem et al., 2007]. The most known, and well characterized pro-angiogenic factor is the vascular endothelial growth factor (VEGF), which plays a central role in angiogenesis both in embryos and in adult organisms; it acts stimulating angiogenesis phases and promoting endothelial cells survival. VEGF binds two different tyrosin-kinase receptors, VEGFR-1 and VEGFR-2, the second one being the one more involved in endothelial cells activation and angiogenesis. VEGFR-2 activates the protein kinase B (PKB), inhibiting apoptosis, and the mitogen activated protein kinases (MAPK), thus stimulating proliferation. Due to the reduced growth factors levels in diabetic peri-lesional tissues, and to the increase in ROS (which impair endothelial cells and fibroblasts metabolism), wound healing process is impaired [Peplow and Baxter, 2012].

MicroRNA expression in diabetic wounds

Recently, new mechanisms involved in wound healing regulation and impairment had been unfolded; particularly, diabetic patients showed an increase in expression of several micro-RNAs (miRNAs). miRNAs are short non-coding RNAs (single strand, 22nt length) which act as post-

transcriptional regulators by binding the complementary 5'UTR of target mRNAs, thus inhibiting translation and promoting the target mRNA degradation.

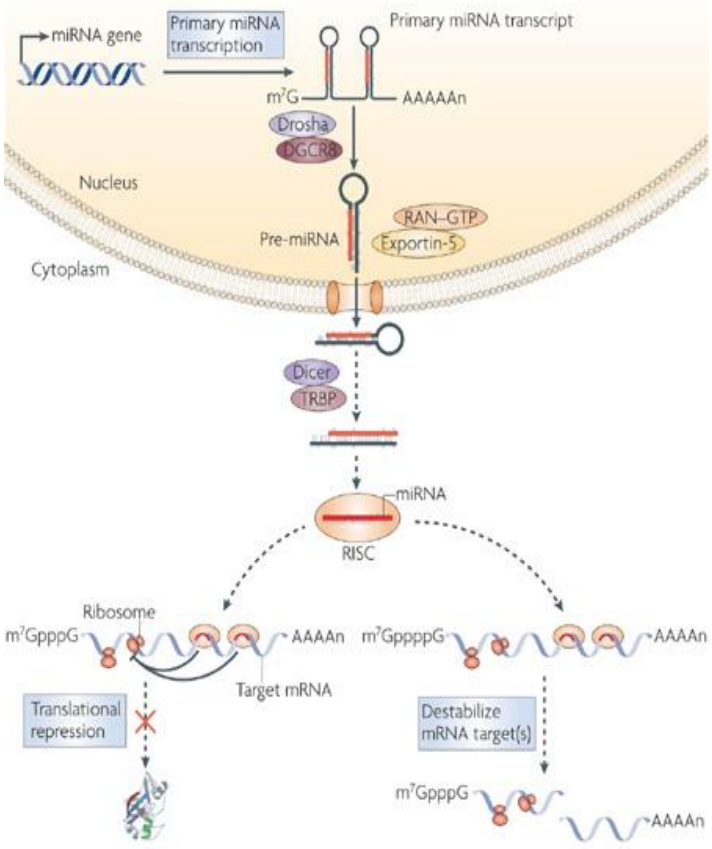

miRNAs can bind several target mRNAs, thus orchestrating a complex regulation in several physiological and pathological conditions, such as inflammation, atherosclerosis, vasculitis, endothelial cells apoptosis [Leeper and Cooke, 2011].

It has been shown that miRNA-15b (miR-15b) is a negative modulator in angiogenesis, as well as miR-200b. The first one (miR-15b) binds VEGF and HIF-1a mRNA, thus determining a reduced production of this key pro-

angiogenic mediators. In an in vivo model of wound healing, diabetic mice showed dramatically increase in miR-15b concentration in perilesional tissues, coupled with a reduced expression of its target genes (VEGF and HIF-1a) [Xu et al., 2014].

On the other hand, miR-200b targets, among other mRNAs, the one codifying for VEGFR2. Experimental evidence show that miR-200b downregulation lead to an improvement in angiogenetic process, ameliorating the wound healing process [Chan et al., 2012]. miRNAs inhibition is a useful tool to perform functional experiments, but it has been also proposed, and it's actually used, as experimental therapeutic strategy.

One way to achieve specific miRNAs inhibition is to target them with short anti-sense nucleic acid complementary to each target miRNA.

These molecules, called antagomiRs, can be used in vivo, and achieve a better affinity for the target, they had been modified in several ways. The most common and efficient modified antagomiRs are the ones called LNAs (locked nucleic acids), which allow to target more than one miRNA simultaneously and have high affinity for the target [Laganà et al., 2014]. This class of antagomiRs carry two methyl groups in 2'-oxygen and 4'-

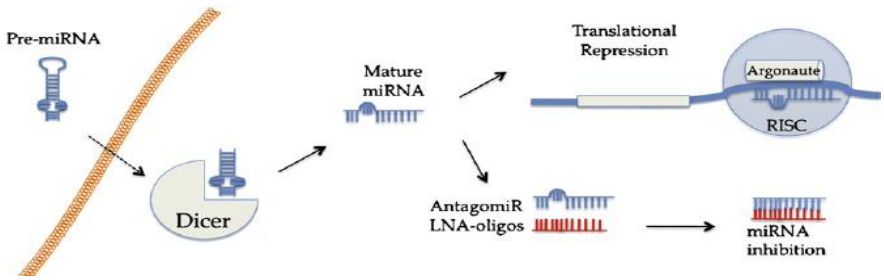

carbon, forming a cyclic structure; this allow the LNAs to did not change conformation (by keto-enolic tautomery), and increase the affinity for the target, decreasing also toxicity [Ishida and Selaru, 2013].

Several studies already showed that antagomiRs can be succesfully used as experimental therapeutic strategy, to rescue the pathology-associated molecular pathway affected by miRNAs overexpression [Laganà et al., 2014].

Taken together, these observations let us to consider the antagomiRs-based miR-15b and miR-200b targeting as therapeutic option to improve wound healing in leptin receptor-knock out diabetic mice. The most effective, high-affinity anti-miRNA oligonucleotides designs rely on highly-modified, synthetic oligonucleotide chemistries as locked nucleic acids (LNA). LNA contain a methylene bridge between the 2'-O and 4'C of ribose to "lock" it into a configuration which is optimal for hybridization. LNA are also highly resistant to nuclease degradation, thus are ideal for in vivo use. Consequently, LNA-based anti-miRNA show higher anti-miR activity at lower doses compared with the equivalent antagomir [Obad et al., 2011].

Relaxin

Relaxin (RLX) is a peptide hormone of the insulin super-family that has a long history as a reprouctive hormone since its discovery in 1926 [Kong et

al., 2010]. Like insulin, relaxin is a 6 kDa protein processed from a pre-proform to the mature hormone containing A and B peptide connected by two inter-chain disulfide bridges, and one inter-chain disulfide within the A chain. Several relaxin-like peptides exist. Two relaxin genes are present in humans, encoding protein known as H1 and H2 relaxin, but only H2 relaxin is known to circulate. Relaxin has been shown to induce VEGF expression and angiogenesis selectively at wound sites in an experimental in vitro model [Unemori et al., 2000]. Furthermore relaxin may also increase the expression of endothelial nitric oxide synthase (eNOS), thus modulating nitric oxide (NO) production. Besides angiogenesis, relaxin may also modulate collagen synthesis and extracellular matrix homeostasis: in fact it increases expression of matrix metalloproteinases (MMP) and degrades collagen, thus antagonizing the exaggerated fibrosis of the wounds (anti-scarring effect) [Mookerjee et al., 2005].

All these experimental observations make relaxin a candidate rationale treatment to speed up wound closure. Indeed an intraperitoneal administration of a crude preparation contained porcine relaxin improved wound healing and increased tensile strength in a rodent model [Beiler et al., 1960] and recombinant H2 relaxin enhanced wound healing and prevented scar formation in a pig excision wound model [Stewart, 2009]. However the

effects of relaxin in the diabetes impaired wound healing have not been fully investigated.

Aim of our studies was to determine whether angiogenetic process could be pharmacologically induced, by using relaxin or antagomirs administration, to promote and improve impaired wound healing in genetically diabetic mice [Altavilla et al., 2001; Galeano et al., 2003].

Materials and Methods - Relaxin experiment

Animals

All animal procedures were in accordance with the Principles of Laboratory Animal Care (NIH publication no.85-23, revised 1985), authorized by our National Institution, and in accordance with ARRIVE guidelines [Kilkenny et al., 2010]. Genetically diabetic female (30-35g) C57BL/KsJ-m+/+*Lept*^{db} mice (db^{+}/db^{+}) and their normal littermates (22-25g) ($db^{+/+}m$) were obtained from Jackson Laboratory (Bar Harbor, ME, USA). Animals were 10 weeks old at the start of the experiments. During the experiments the animals were maintained one per cage, under controlled environmental conditions (12hour light-dark cycle, 23°C), and provided with standard food and water ad libitum. After general anesthesia with sodium pentobarbital (80 mg/kg/i.p.), hair on the back was shaved and two parallel 4-cm incisions were produced with the use of a scalpel (Figure 1A), on the back of all mice as previously described [Altavilla et al., 2011].

In preliminary experiments, relaxin (RLX; IBSA Rizhao-Lanshan, Biochemical Products, Lanshan, China) dose was titrated against the effects on VEGF expression. Normoglycaemic animals (n=24), following skin incision, were implanted sub-cutaneously with osmotic pumps delivering different RLX concentrations (6.25, 12.5, 25, and 50µg/mouse/day). The

pumps were implanted on the neck right above the mid-scapular line (Figure 1A) and the treatments lasted six days. This experiment identified 25µg/mouse/day of RLX as the optimal dose to be used in the further experiments, indeed the highest dose (50µg/mouse/day) did not show additional improvements.

The animals (n=72) were divided into groups of 6 animals each. Normoglycaemic and diabetic mice, received either RLX (25µg/mouse/day/s.c.) or its vehicle (6µl/mouse/day of 0.9% NaCl) for up to 12 days. Ten animals from each strain were killed after 3, 6 and 12 days after surgery, and the wounds removed by using a scalpel to cut the shape of an ellipse around the lesion. Of the two wounds, one was used for nitric oxide products (only at day 6) or tensile strength (only at day 12), and the other one sectioned for the other analysis as shown in Figure 1A. All animals sacrificed at day 12 were also tested for glycemic blood levels, by using a colorimetric glucose oxidase assay (One-Touch; Lifescan, Milpitas, CA, USA).

To better understand if the angiogenetic or the vasculogenetic pathway were affected by relaxin, two additional groups (n=7 for each group) of diabetic animals underwent wounding and received RLX (25µg/mouse/day/s.c.) together with the anti-VEGF murine antibody (10mg/kg/i.p. daily; Abcam, Cambridge, UK) or with the anti CXCR4 antibody (0.4mg/kg/i.p. daily;

Enzo Lifescience, Lausen, Switzerland). Additional (n=36) normoglycaemic (n=18) and diabetic mice (n=18) were subjected to wounding, implanted with pumps and used to investigate the time needed to complete wound closure.

Real Time PCR for VEGF and SDF-1α

Briefly, total RNA was extracted from wound samples, and quantified as previously described [Galeano et al., 2011]. RNA was reverse transcribed to cDNA and used to quantitate the amount of VEGF and SDF-1α mRNA by real time polymerase chain reaction (Real-Time PCR), β−actin was used as endogenous control. The results were expressed as the n-fold difference relative to normal controls (relative expression levels).

Determination of eNOS by Western blot analysis

eNOS expression was evaluated at day 6, by Western Blot, as previously described [Galeano et al., 2006]. Primary antibodies for eNOS and phospho-eNOS (Ser1177) were purchased from Chemicon, (Temecula, CA, USA) and Cell Signaling (Danvers, MA, USA) respectively. Secondary peroxidase conjugated antibodies were obtained by Pierce (Rockford, IL, USA). The protein signals were quantified by scanning densitometry, using a bio-image analysis system (Bio-Profil Celbio, Milan, Italy), and were expressed as

integrated intensity in comparison with β-actin (Cell Signaling) measured on stripped blots.

Determination of NO_2^-/NO_3^-

At day 6 a piece of wound samples were removed and frozen in liquid nitrogen until use. NO products were determined in wound lysates using the Griess reaction, as previously described [Galeano et al., 2006]. All samples and standards, were assayed in triplicate. Data were expressed as mean ± SD of NO_2^-/NO_3^-.

Determination of VEGF in wounds

The amount of VEGF in wounds was determined at 3, 6 and 12 days, by a commercially available VEGF-specific ELISA assay kit (R&D Systems, Minneapolis, MN, USA) as previously described [Altavilla et al., 2011]. The amount of VEGF was expressed as picograms per milligram of protein.

Histologic examination and time to complete wound closure

Wound samples were fixed in 10% neutral buffered formalin, and processed as previously described [Altavilla et al., 2011]. All slides were examined by a pathologist blinded to the previous treatment, by means of an eye-piece grid under the microscope from x20 to x100 magnification. The following

parameters were evaluated and scored: re-epithelialization, dermal matrix deposition and regeneration, granulation tissue formation and remodeling. The histological specimens were evaluated according to the score reported in the literature concerning wound healing in experimental models [Altavilla et al., 2011; Galeano et al., 2001, 2006, 2008, 2011].

Time to complete wound closure, evidenced by a closed linear healing ridge, was monitored as previously described [Galeano et al., 2008].

Immunohistochemistry for VEGFR1, VEGFR2, VE-Cadherin, CD-31, CD-34 and MMP-11

Paraffin-embedded tissues were sectioned (5μm), re-hydrated, and antigen retrieval was performed using 0.05M sodium citrate buffer. Slides were incubated overnight with primary antibody to detect CD-31, CD-34, MMP-11, vascular endothelial (VE)-cadherin, VEGFR-1 (all from Abcam), and VEGFR-2 (Cell Signaling) as previously described [Galeano et al., 2008]. DAB (3-3' Diaminobenzidine, Sigma, St Louis, MO) was used to reveal the reaction and counterstain was performed with haematoxylin where needed.

To assess new blood vessel formation, microvessel density (MVD) was estimated after CD-31 staining. Briefly, three hot spots or areas with the highest visible blood vessel density (marked by the vessel marker) per section were selected, in the dermis just proximal to the wound site, and the

number of small caliber blood vessels having a visible lumen were counted per high-power field (x40 magnification) by three pathologists blinded to the samples. To assess positive CD-34, VEGFR-1, VE-cadherin and VEGFR-2 staining six areas per section were randomly selected in the dermis and the positive endothelial cells were counted per high-power field (x40 magnification) by three pathologists blinded to the samples. To evaluate positive MMP-11 staining five areas per section were randomly selected in the sub-epithelial tissue and positive spots were counted per high-power field (x40 magnification) by three pathologists blinded to the samples. For negative controls, the primary antibodies were replaced by citrate buffer (pH 6.0).

Breaking strength

At day 12, the maximum load (breaking strength) tolerated by wounds was measured blindly on coded samples using a calibrated tensometer (Sans, Milan, Italy) as previously described [Galeano et al., 2008]. The ends of the skin strip were pulled at a constant speed (20 cm/min), and breaking strength was expressed as the mean maximum level of tensile strength in newton (N) before separation of wounds.

Statistical analysis

All data were expressed as means and standard deviations (mean ± SD). Comparisons between different treatments were analysed by one-way ANOVA followed by Tukey's multiple comparison test. In all cases, a probability error of less than 0.05 was selected as the criterion for statistical significance. Graphs were drawn using GraphPad Prism (version 5.0 for Windows).

Materials and Methods - Antagomirs experiment

Antagomirs design

Antagomirs have been designed in order to be reverse complementary to the respective miRNAs (miR-15b and miR-200b); the sequence of both miR-15b and miR200b has been obtained from mirbase.org: miR-15b: 5'-UAGCAGCACAUCCUGGUUUACA- 3'; miR-200b: 5'-CAUCUUACUGGGCAGCAUUGGA-3'. Considering these sequences we designed the two antagomirs: anti-miR-15b: 5'-UGUAAACCAGGAUGUGCUGCUA-3'; anti-miR-200b: 5'-UCCAAUGCUGCCCAGUAAGAUG-3'. Antagomirs have been purchased by Exiqon (Denmark), shipped as dry powder and re-suspended in RNAse-free water to reach a 25nM final concentration.

Animals and experimental procedures

All the animal procedures have been performed following the Directive 63/2010/EU on the protection of animals used for scientific purposes, have been approved by our local Ethics Committee and were in accordance with the ARRIVE Guidelines [Kilkenny et al., 2010].

C57BL/KsJ-m+/+ Leptdb (db+/db+) female diabetic mice (n=68; 10 weeks old at the beginning of the experiment) have been purchased by Jackson

Laboratory (Bar Harbor, ME, USA). Animals have been kept in controlled environmental conditions (12h day-night cycles, 23-24 °C), with food and water ad libitum, and the proper enrichment.

After general anesthesia (ketamine and xylazine 80 and 10 mg kg-1 respectively i.p.), animals were shaved on the back, and the skin cleaned with iodine solution. Incisional wounds were performed as follow: two longitudinal incisions (3cm in length) were produced and then sutured with 4-0 silk, as previously reported [Bitto et al., 2013; Bitto et al., 2014]. Animals (10 in each group) were randomized to receive a single dose of anti-miR-15b (10mg/kg in 0,9% NaCl); anti-miR-200b (10mg/kg in 0,9% NaCl); or both anti-miR-15b and anti-miR-200b, or vehicle alone (0,9% NaCl). Antagomirs have been administered perilesionally in a final volume of 200 μl.

Before killing blood glucose levels have been tested with the Multicare instrument (2Biological Instruments, Besozzo, Italy) with a detection range of 25-500mg/dl. Five mice from each group have been killed 7 and 14 days after the surgical procedure. One of the incisions has been collected to perform molecular analysis, the other one to perform histology and immunohistochemistry.

To evaluate the time of complete wound closure we performed an excisional wound on additional 28 mice, in brief, a circular piece (1cm diameter) of cutaneous tissue was removed, from the shaved back of diabetic animals

using a biopsy punch. Animals have been then randomized (7 in each group) to receive the same above reported treatments and sacrificed at the time of complete wound closure.

RT-qPCR

Total RNA was extracted from skin samples (70 mg) using Trizol reagent (Thermo Fisher Scientific, Waltham, MA, USA), following the manufacturer's protocol and was quantified with a spectrophotometer (NanoDrop Lite, Thermo Fisher Scientific). Reverse transcription was carried out using 1µl of RNA by using the SuperScript® VILOTM cDNA synthesis kit (Thermo Fisher Scientific) and random primers, following the manufacturer's protocol. 1µl of total cDNA was used to quantify VEGF-A, Angiopoietine-1, TEK e VEGFR2 by Real-Time qPCR, using β-actin as endogenous control. Reactions have been carried out in singleplex in 96-well plates using the TaqMan Universal PCR master mix and TaqMan probes (Applied Biosystems).

PCR reaction was monitored by using the QuantStudio 6 Flex (Applied Biosystems), and results were quantified by the 2-ΔΔCt method for either target and endogenous gene. As calibrator we used unwounded skin from diabetic animals.

Histologic examination and time to complete wound closure

Wound samples were fixed in 10% neutral buffered formalin, and processed as previously described (Bitto et al., 2014). All slides were examined by a pathologist blinded to the previous treatment, by means of an eye-piece grid under the microscope from x20 to x100 magnification. The following parameters were evaluated and scored: re-epithelialization, dermal matrix deposition and regeneration, granulation tissue formation and remodelling. The histological specimens were evaluated according to the score reported in the literature concerning wound healing in experimental models [Bitto et al., 2014].

Time to complete wound closure, evidenced by a closed linear healing ridge, was monitored as described previously [Bitto et al., 2014].

Immunohistochemistry

Paraffin-embedded tissues were sectioned (5μm), re-hydrated, and antigen retrieval was performed using 0.05M sodium citrate buffer as previously described (Bitto et al., 2013). Slides were incubated overnight with primary antibody to detect CD-31 (Abcam), and VEGFR-2 (Cell Signaling). DAB (3-3' Diaminobenzidine, Sigma, St Louis, MO) was used to reveal the reaction and counterstain was performed with haematoxylin where needed.

To assess new blood vessel formation, microvessel density (MVD) was

estimated after CD-31 staining. Briefly, three hot spots or areas with the highest visible blood vessel density (marked by the vessel marker) per section were selected, in the dermis just proximal to the wound site, and the number of small caliber blood vessels having a visible lumen were counted per high-power field (x40 magnification) by three pathologists blinded to the samples.

Breaking strength

At day 12, the maximum load (breaking strength) tolerated by wounds was measured blindly on coded samples using a calibrated tensometer (Sans, Milan, Italy) as previously described [Bitto et al., 2013]. The ends of the skin strip were pulled at a constant speed (20 cm/min), and breaking strength was expressed as the mean maximum level of tensile strength in newton (N) before separation of wounds.

Statistical analysis

All data were expressed as means and standard deviations (mean ± SD). Comparisons between different treatments were analysed by one-way ANOVA followed by Tukey's multiple comparison test. A probability error of less than 0.05 was selected as the criterion for statistical significance. Graphs were drawn using GraphPad Prism (version 5.0 for Windows).

Results - Relaxin experiment

Identification of the RLX dose

Normoglycaemic animals were treated for 6 days after wounding with RLX at different concentrations (6.25, 12.5, 25 and 50µg/mouse/day) in order to identify the optimal dose to be used in further experiments. Figure 1B shows that the most effective RLX dose in increasing VEGF expression was 25µg/mouse/day. A greater dose did not further increase VEGF expression.

VEGF expression and protein content in wounds

In the wounds of non-diabetic animals, a strong induction of VEGF mRNA (Fig. 1C) was found at day 3 and 6 when compared with basal values (uninjured skin= 0.05 ±0.001 nfold/ßactin; $P<0.001$). VEGF protein levels in uninjured skin from non-diabetic and diabetic mice were very low (results not shown). In the wounds of non-diabetic animals, VEGF content increased at days 3 and 6 compared with basal values (Fig. 1D). Thereafter, VEGF expression and protein levels declined at day 12. Administration of RLX enhanced VEGF mRNA and protein content at day 3 and 6 in normoglycaemic animals (Fig.1C, D).

Wounds from diabetic mice showed a markedly reduced expression and protein levels of VEGF when compared with non-diabetic ones at days 3 and

6 following surgery. VEGF mRNA and protein levels were still significantly detectable at day 12 in diabetic mice (Fig. 1C, D). Daily treatment with RLX enhanced VEGF expression and protein levels at days 3 and 6, thus restoring the disturbed pattern of VEGF secretion (Fig. 1C, D).

SDF1-α expression in wounds

In the wounds of non-diabetic animals, SDF1-α mRNA increased significantly at days 3 and 6 when compared with basal values (uninjured skin= 0.02±0.005 nfold/ßactin; $p<0.001$). SDF1-α expression remained sustained at day 12 (Fig. 1E). Administration of RLX slightly, but not significantly enhanced SDF1-α mRNA at day 3 and 6 in normoglycaemic animals.

Wounds from diabetic mice showed a markedly reduced expression of SDF1-α when compared with non-diabetic ones at day 6 following surgery (Fig. 1E). Daily treatment with RLX augmented SDF1-α levels, thus restoring the impaired pattern of SDF1-α mRNA expression (Fig. 1E).

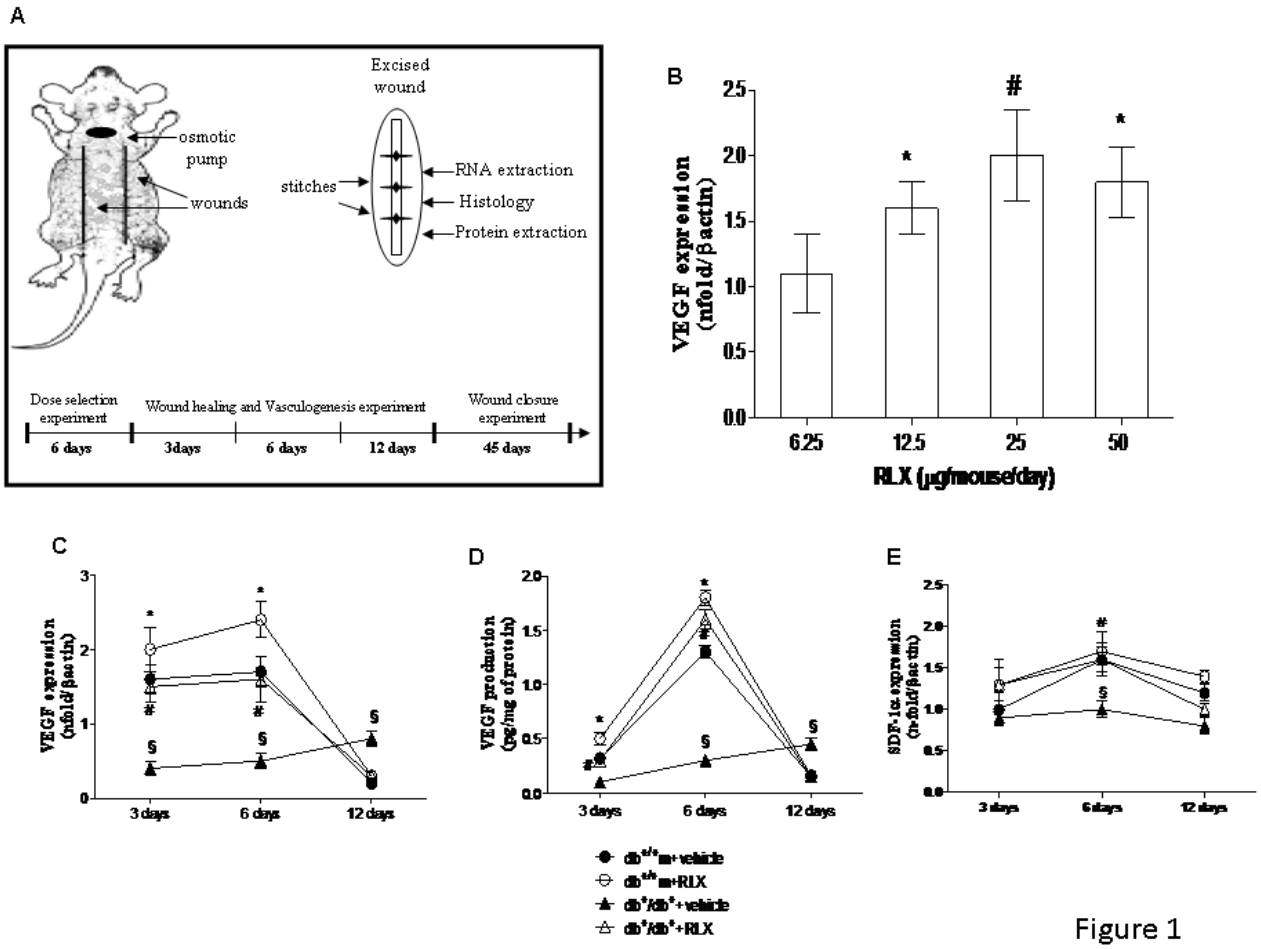

Figure 1

Expression of eNOS in wounds

Uninjured skin specimens showed a very low content of phospho-eNOS (0.7±0.04 and 0.4±0.06 integrated intensity in normoglycaemic and diabetic mice, respectively). Wounding enhanced expression of phospho-eNOS in both strains of animals at day 6 (Fig. 2A), but this expression was significantly lower in diabetic animals. In wound treated with RLX, a greater

increase in phospo-eNOS was detected in both non-diabetic and diabetic animals compared with vehicle treated animals (Fig. 2A).

NO products in wounds

Wounding produced a remarkable increase in NO_2^-/NO_3^- content compared with control uninjured skin at day 6 (1.3±0.4 and 0.8±0.04 nmol/g of tissue in normoglycaemic and diabetic mice, respectively). However NO_2^-/NO_3^- levels were significantly reduced in the wounds of diabetic animals. A significant higher enhancement in wound NO products was observed in RLX administered diabetic and non-diabetic mice compared with vehicle treated animals (Fig. 2B).

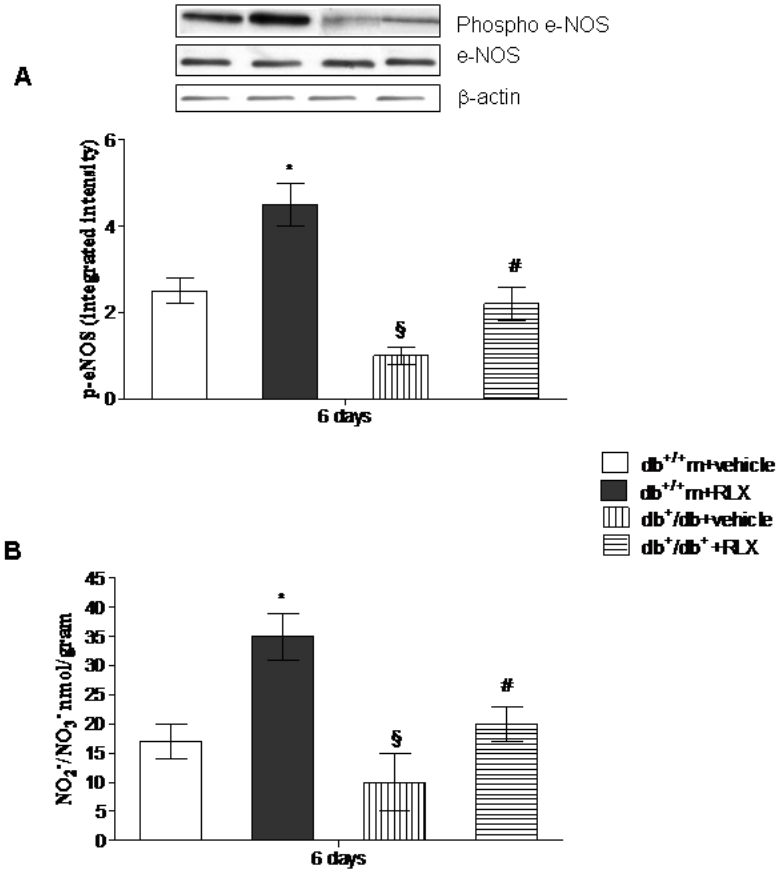

Figure 2

Histology

Figure 3 shows the histological scores (A) and representative histological pictures (B, C, D and E) of the several experimental groups at day 12. In normoglycemic animals dermis remodeling and wound closure process were complete (Fig. 3A, B). However the administration of RLX qualitatively improved wound healing (Fig. 3A, C).

Diabetic wounds of mice administered with vehicle at day 12 showed poor- to mild reepithelialization with partially organized granulation tissue (Fig. 3A, D). In contrast, moderate to complete reepithelialization and well-formed granulation tissue were observed in the diabetic wound of mice treated with RLX (Fig. 3A, E).

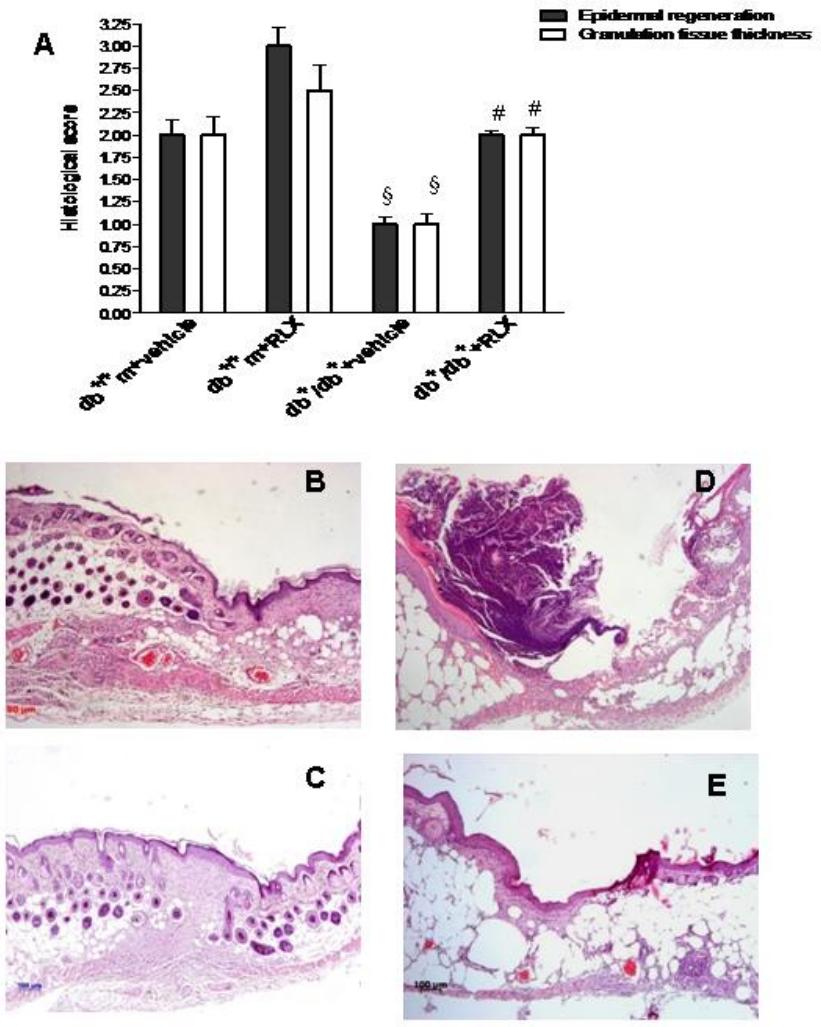

Figure 3

Wound closure

The time to complete wound closure was indicated by a closed linear ridge, with no open areas between stitches. Complete skin normalization in untreated normoglycaemic animals occurred at day 23±3 after wounding and RLX did not modify this parameter (Fig. 4). Wound closure in diabetic animals was observed at day 38±3 after the surgical procedure and RLX markedly reduced the time to complete wound closure (Fig. 4). A concomitant treatment with antibodies raised against either VEGF or

CXCR4 abated this effects, thus confirming that both VEGF and SDF1-α mediates the beneficial relaxin effects on wound healing.

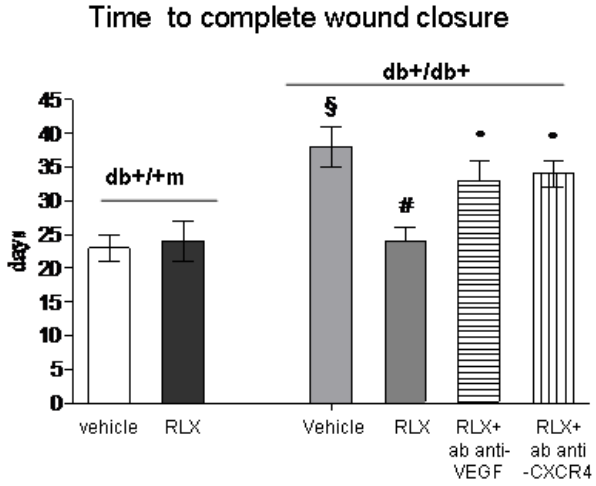

Figure 4

Evaluation of new blood vessel formation

CD-31 immunostaining was investigated at day 12 to confirm neo-vessel formation (Fig. 5). In fact, this protein represents an highly specific marker for endothelial cells. Positive staining was present in the wounds from vehicle administered non diabetic animals (Fig. 5C). This staining appeared markedly reduced in the wounds from diabetic animals injected with vehicle (Fig. 5A). Administration of RLX augmented CD-31 immunostaining in both strains of mice (Fig. 5B, C). The effect was remarkable in diabetic wounds where the positive staining was mostly localized in small vessels and capillaries (Fig. 5B). Using the images obtained from CD-31 staining, the tissue samples were assessed for micro-vessel density (Fig. 5C). Treatment with RLX markedly increased micro-vessel density (MVD) in both non-diabetic and diabetic animals (Fig. 5C).

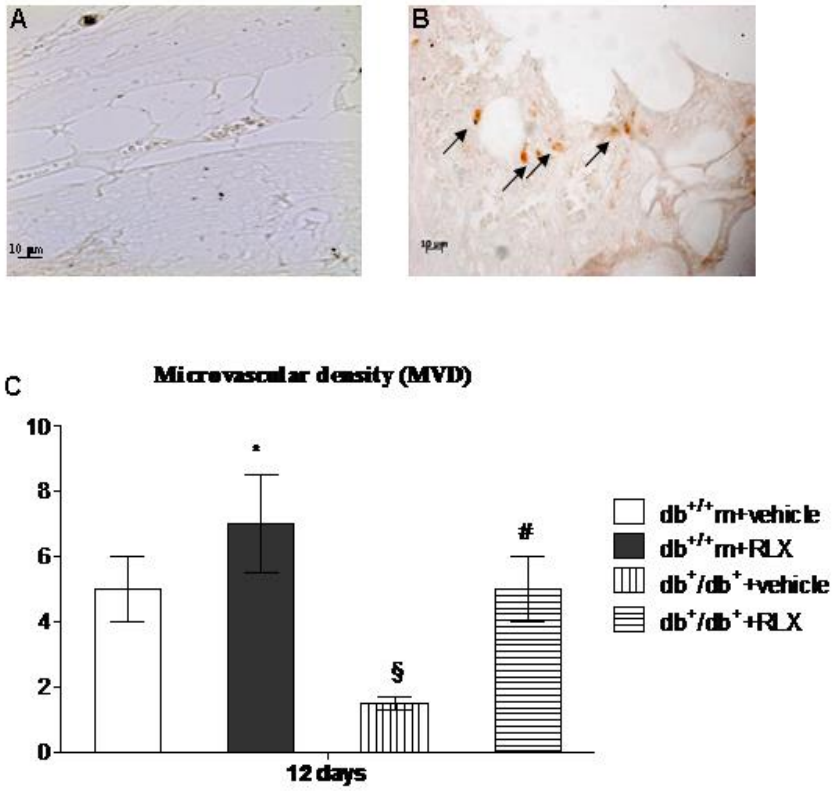

Figure 5

Assessment of CD-34 and VEGF-R1 immunostaining

To confirm neo-angiogenesis, CD-34 and VEGF-R1 immunostaining was also studied at day 12 (Fig. 6). Positive staining was evident in the wounds from vehicle injected non diabetic animals (Fig. 6C and F). This staining was significantly reduced in the wounds from diabetic animals injected with

vehicle (Fig. 6A, D). Administration of RLX enhanced CD-34 (Fig. 6B, C) and VEGF-R1 (Fig. 6E, F) immunostaining in both strains of mice. In RLX-treated diabetics a marked staining in the sub-epithelial layer was observed, VEGF-R1 in fact exist also in soluble form and the diffuse staining suggest an enhanced production. Figures 6C and 6F represent a quantitative representation of these results.

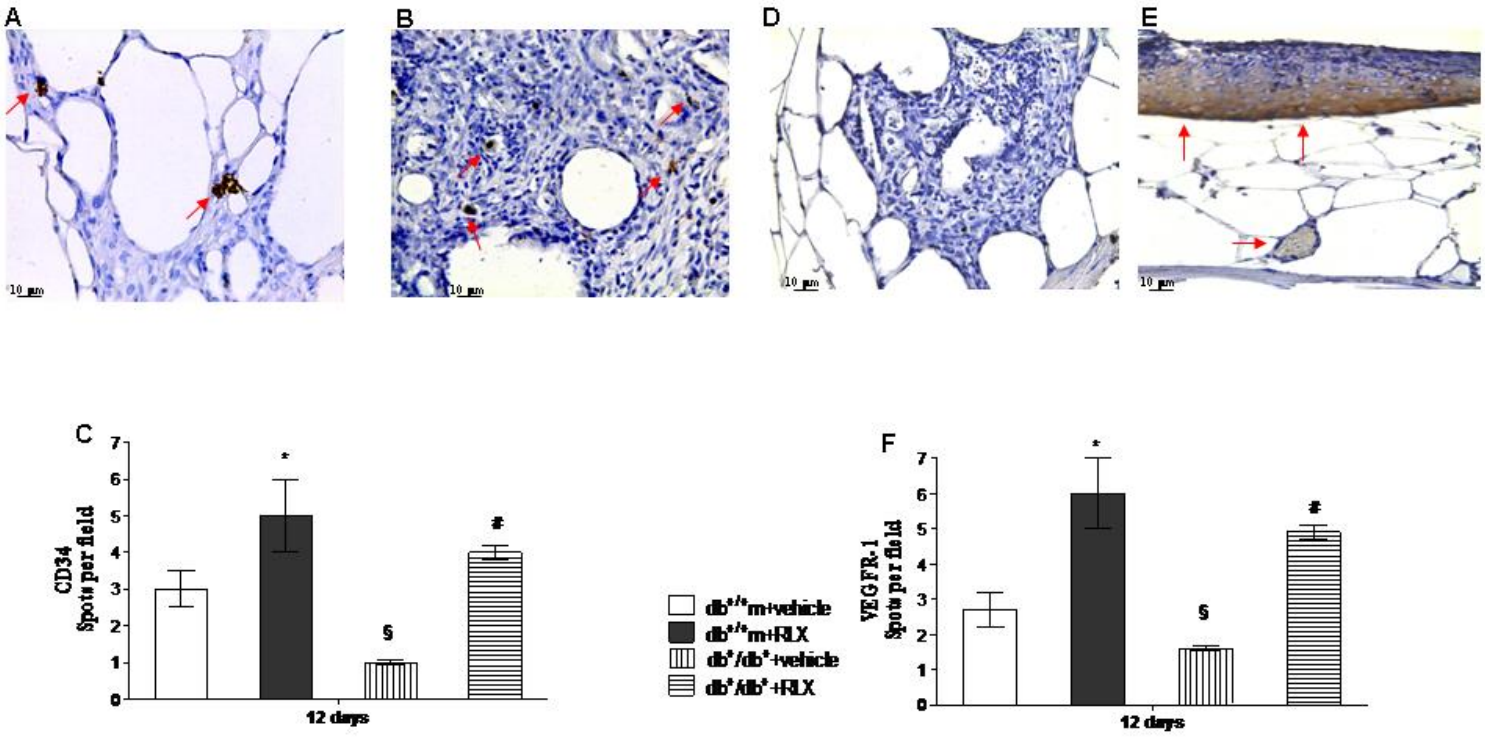

Figure 6

Assessment of VEGF-R2 and VE-cadherin immunostaining

At day 12, immunostaining was performed for VEGFR-2 and VE-cadherin, markers that identify endothelial precursors cells. These cells are not only circulating and bone-marrow derived, but they are also present in subcutaneous adipose tissue. A slight staining for VEGFR-2 (Fig. 7A, C) and VE-cadherin (Fig. 7D, F) was observed in both strains of mice administered with vehicle. Injection of RLX significantly increased VEGFR-2 (Fig. 7B, C) and VE-cadherin (Fig. 7E, F) staining in both non-diabetic and diabetic animals. Figures 7C and F show a quantitative representation of these results.

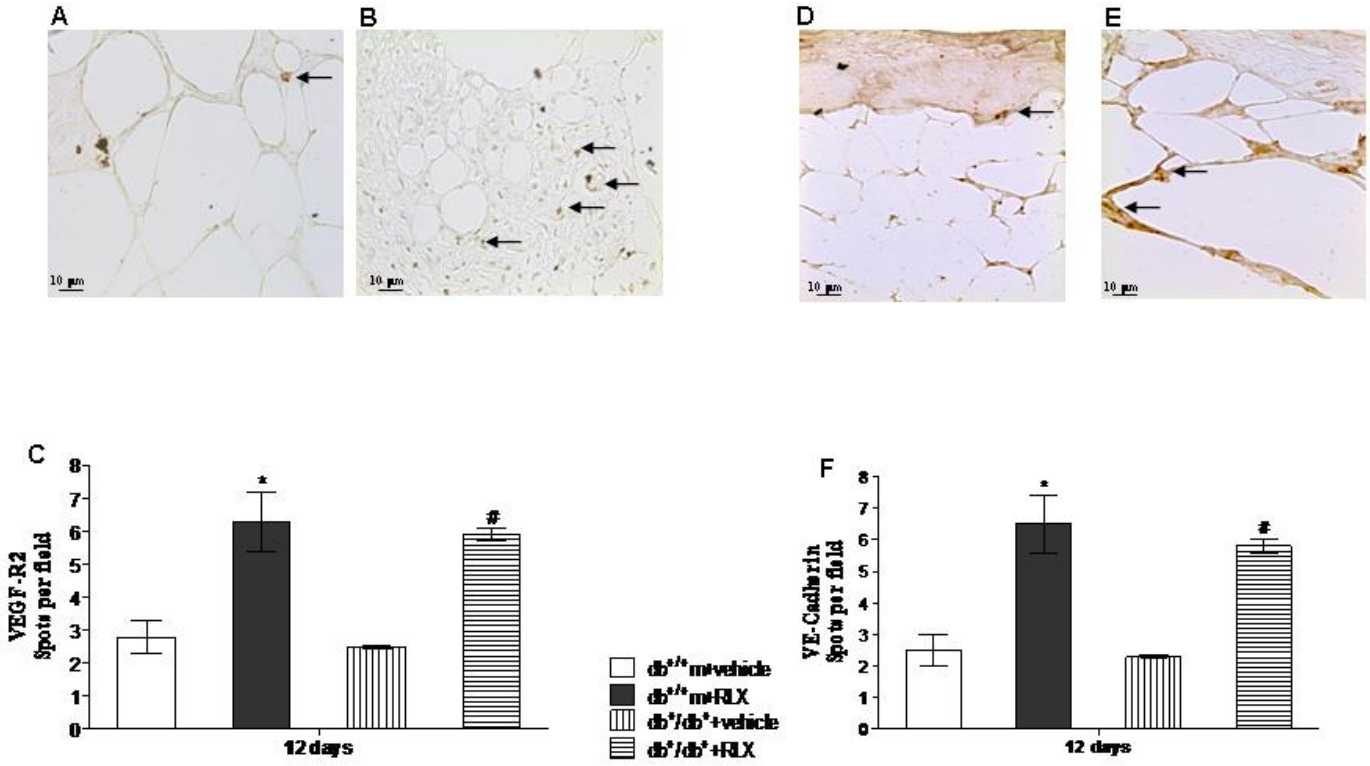

Figure 7

Assessment of MMP-11 immunostaining

To ascertain whether RLX modulates collagen synthesis and extracellular matrix homeostasis, MMP-11 immunostaining was investigated. A slight staining for MMP-11 was evidenced in both strains of mice administered with vehicle (Fig. 8A, C). Injection of RLX significantly augmented MMP-

11 staining in both non-diabetic and diabetic animals (Fig. 8B, C). In this latter group, a strong positive stain was shown in the subepithelial tissue and in endothelial cells from newly formed capillaries, thus suggesting that RLX may antagonize the exaggerated fibrosis of the wounds. Figure 8C shows a quantitative representation of these data.

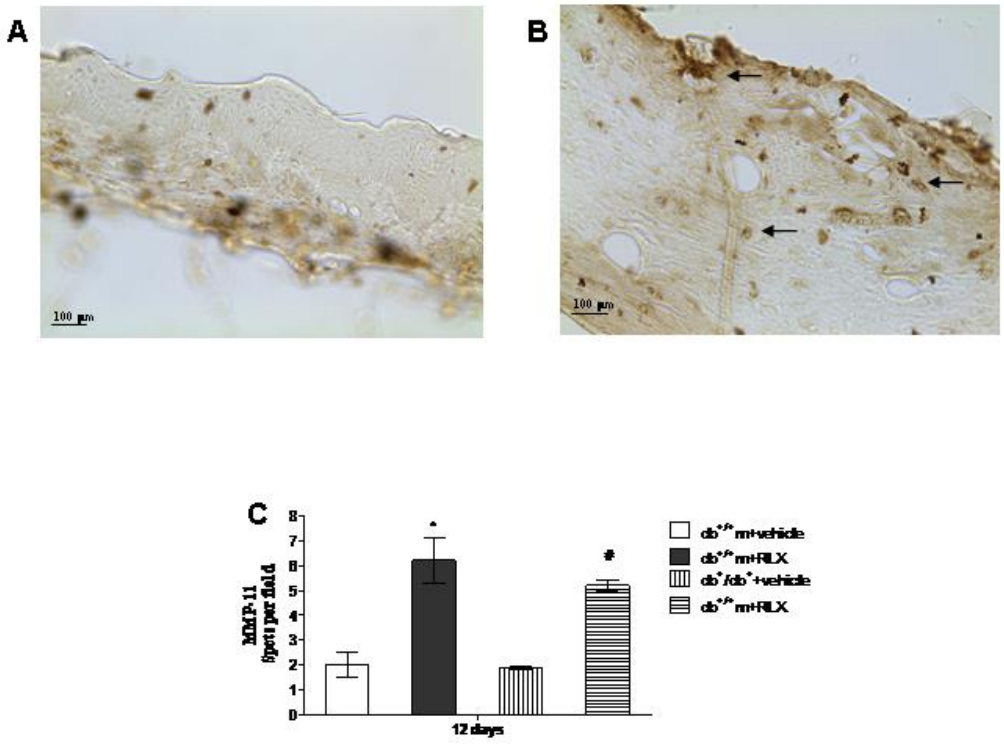

Figure 8

Wound breaking strength and blood glucose levels

Figure 9 shows wound-breaking strength (A) and blood glucose levels (B) for each group at day 12. Wound breaking strength of diabetic mice was significantly lower than that of normoglycaemic animals. Administration of RLX did not significantly change this parameter in non diabetic animals (Fig. 9A). The breaking strength of incisional diabetic wounds of mice treated with RLX was higher than that of diabetic mice treated with vehicle (Fig. 9A).

At the end of the experiment, blood glucose levels (Fig. 9B) in diabetic animals treated with vehicle were 660±32 mg/dl. Blood glucose levels in non-diabetic animals averaged 120±12 mg/dl. RLX administration did not modify glycaemia in non diabetic animals (106±10 mg/dl) but it significantly reduced blood glucose in diabetic animals (490±60 mg/dl).

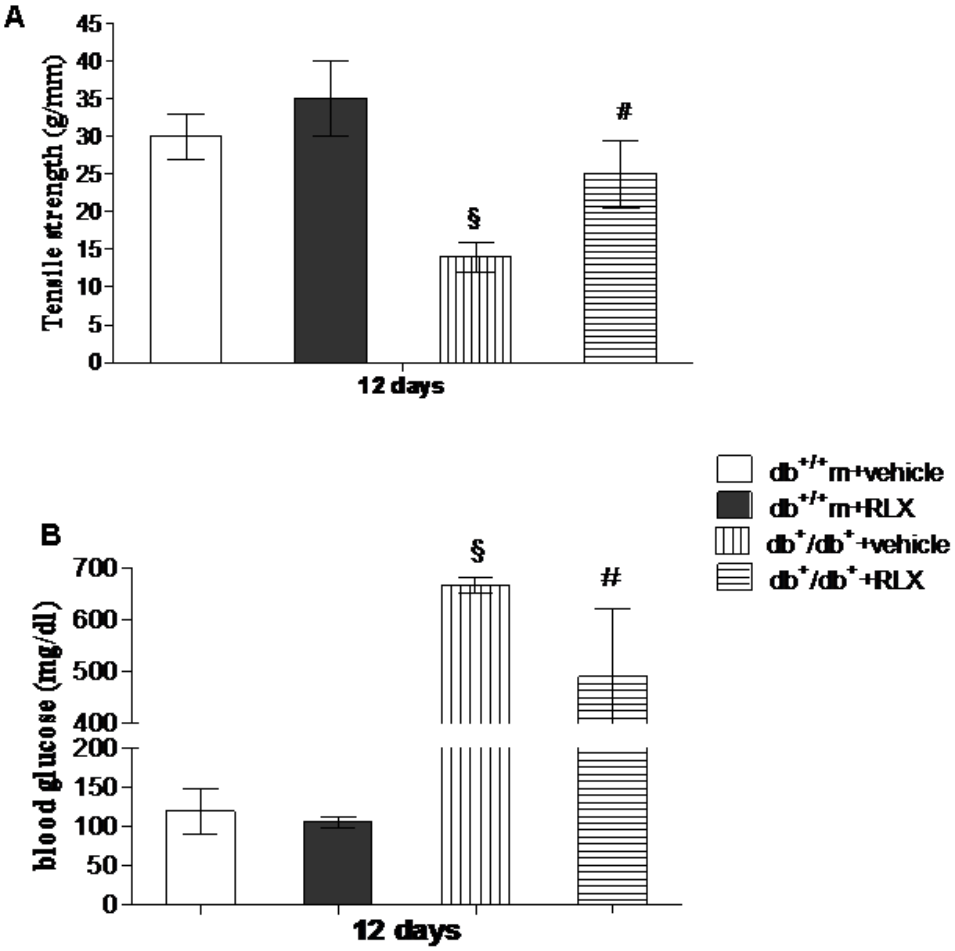

Figure 9

Results - Antagomir experiment

VEGF expression in wounds

Diabetic mice tissue from lesions showed a significant reduction in VEGF mRNAs, compared to normal skin from wild type mice, and un-wounded skin from diabetic mice.

Treating the mice with anti-miR-15b and anti-miR-200b (concomitantly), we observed a non-significant improvement in VEGF mRNA, compared to both the un-wounded skin from diabetic mice, and normal skin from wild type mice (Figure 10A). At 14 days, anti-miR-15b seems to increase VEGF expression, even if in a not-significant way (Figure 10B).

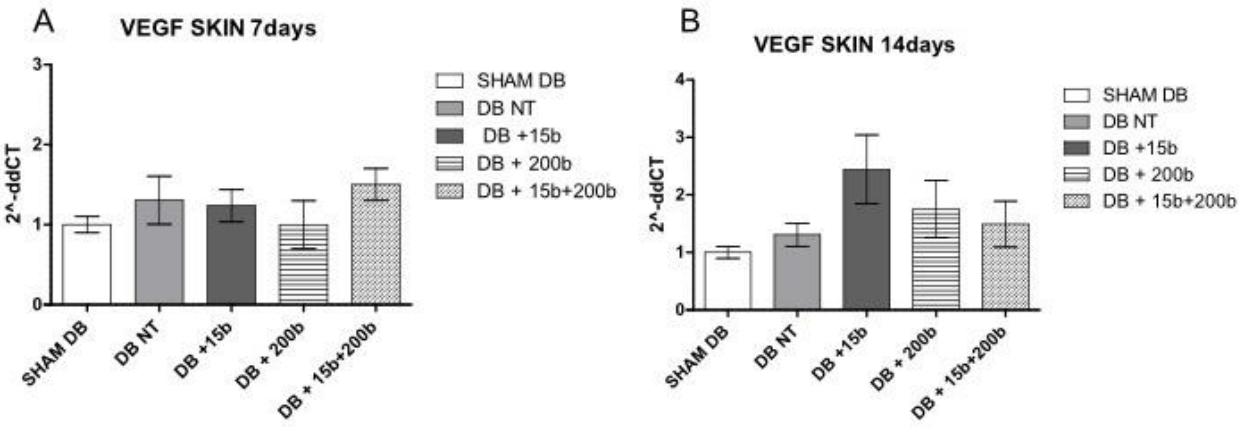

Figure 10

Angiopoietin-1 and TEK (Tie-2) expression in wounds

As well as for VEGF, angiopoietin-1 also appears downregulated, at mRNA level, in wounds from diabetic animals, when compared to unwounded skin

from both diabetic and normal mice. Treatment with anti-miR-15b and anti-miR200b, alone or in combination, did not improve the levels of such mRNA (Figure 11A and 11B). The very same pattern of mRNA expression can be observed at 14 days.

A same pattern of expression was observed for TEK mRNA: downregulated in diabetic wound tissue, compared to normal tissue from diabetic and healthy animals. anti-miR-200b alone, and in combination with anti-miR-15b, increased TEK levels ($p=.0286$ and $p=.05$, respectively) compared to untreated animals; compared to anti-miR-15b treated animals, the increase was significant with both anti-miR-200b alone and combined to anti-miR-15b ($p=0.0079$ e $p=0.0179$, respectively). This suggest that anti-miR-15b did not let the new vessels to reach a mature state (Figure 11).

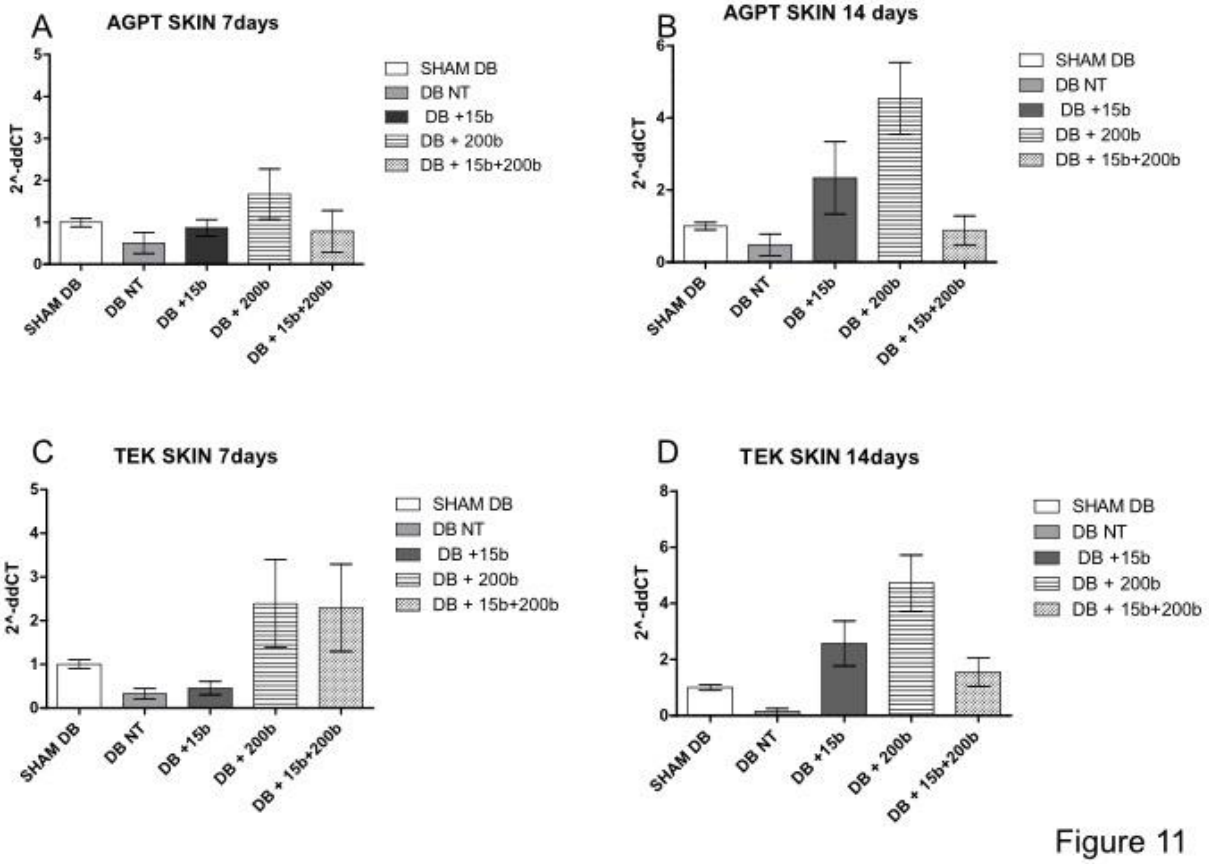

Figure 11

VEGF and VEGFR-2 protein expression in wounds

Untreated diabetic animals showed very low VEGF levels, while anti-miR-15b (alone, and in combination with anti-miR-200b) increased VEGF protein levels in a significative manner (Figure 13). Anti-miR-200b administered alone lead to a non-significant increase in VEGF levels.

On the other hand, VEFR-2 levels were increased in diabetic wound tissues treated with anti-miR-15b, anti-miR-200b, alone and combined together

(Figure 13). Diffuse staining also suggest endothelial progenitor cells presence, a common feature in tissues undergoing to a remodeling phase.

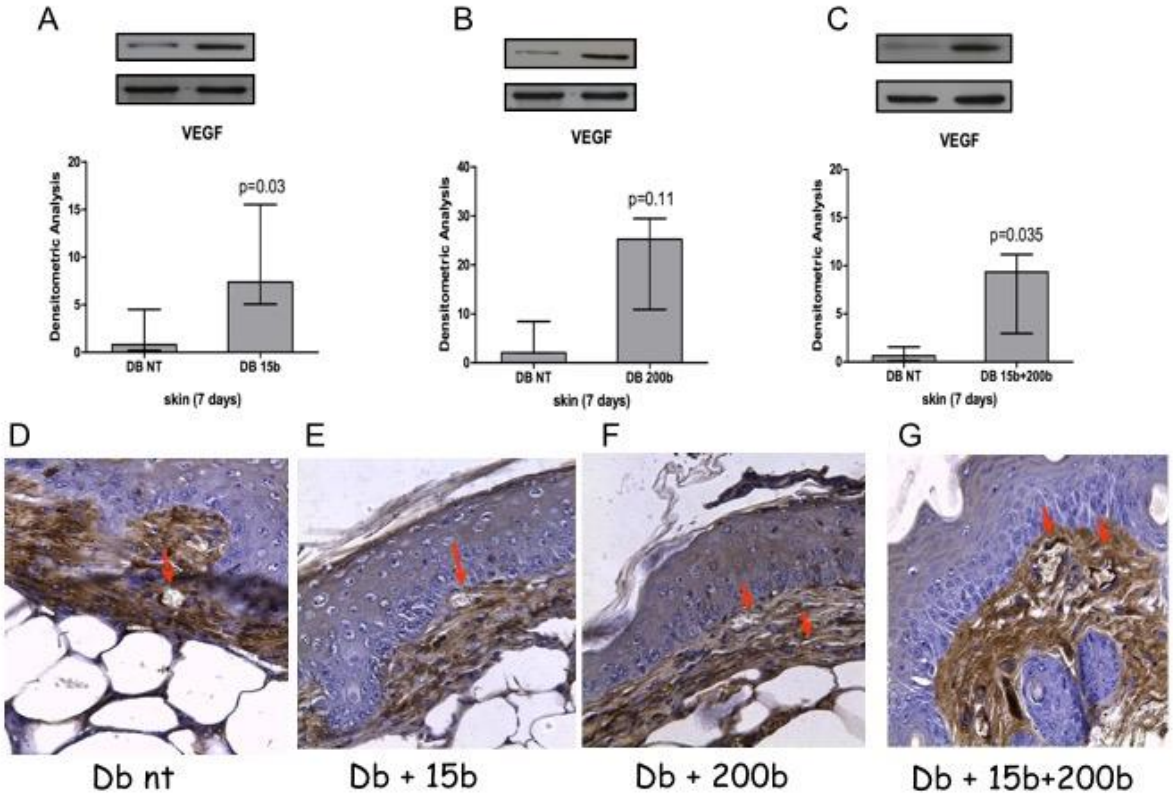

Figure 13

TG2 expression in wound tissue

TG2 promotes the ECM-VEGF binding, which in turn leads to a better activation of VEGFR2. In wound tissue from diabetic mice, TG2 is less expressed; treatment with our anti-miRs, but not in combination, provoked an increase in TG2 levels (Figure 14A-C).

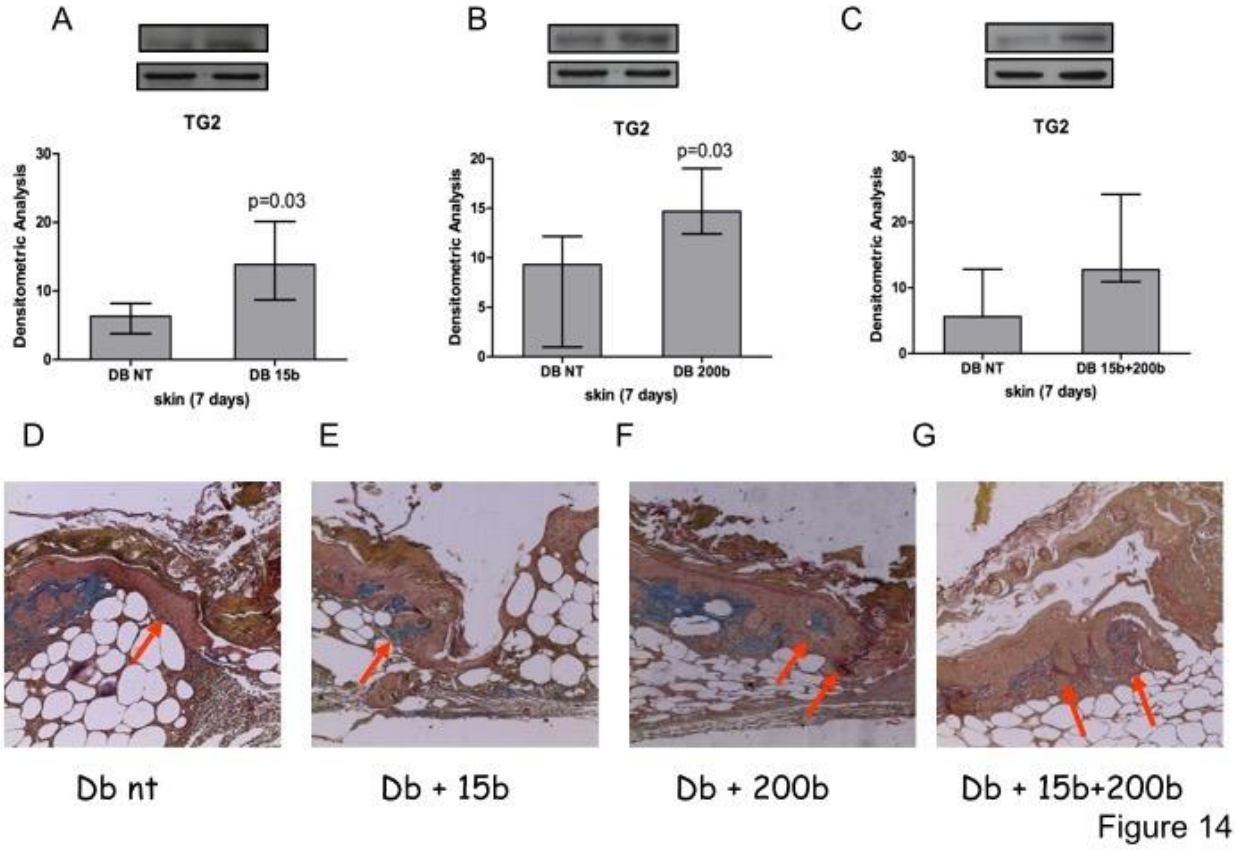

Figure 14

Histology

Untreated diabetic mice 7 days after wound procedure showed an abundant infiltration of inflammatory cells, erythrocytes in perilesional dermal tissue, and hemorrhagic scab. Moreover, epithelial rime was not complete, and most of the histologic samples showed a complete separation between the two epidermal edges. Animals treated with anti-miR-15b showed a decrease inflammatory infiltrate, and a partially closed epidermal edge, while those treated with anti-miR-200b showed a completely restored epithelial edge,

even if the sub were still present, and granulation tissue less abundant. Double-treating the animals with anti-miR-15b and anti-miR-200b, we achieved the best realist in terms of histological features: basal membrane recovered and almost complete granulation tissue retraction (Figure 12, 14D-G and 15).

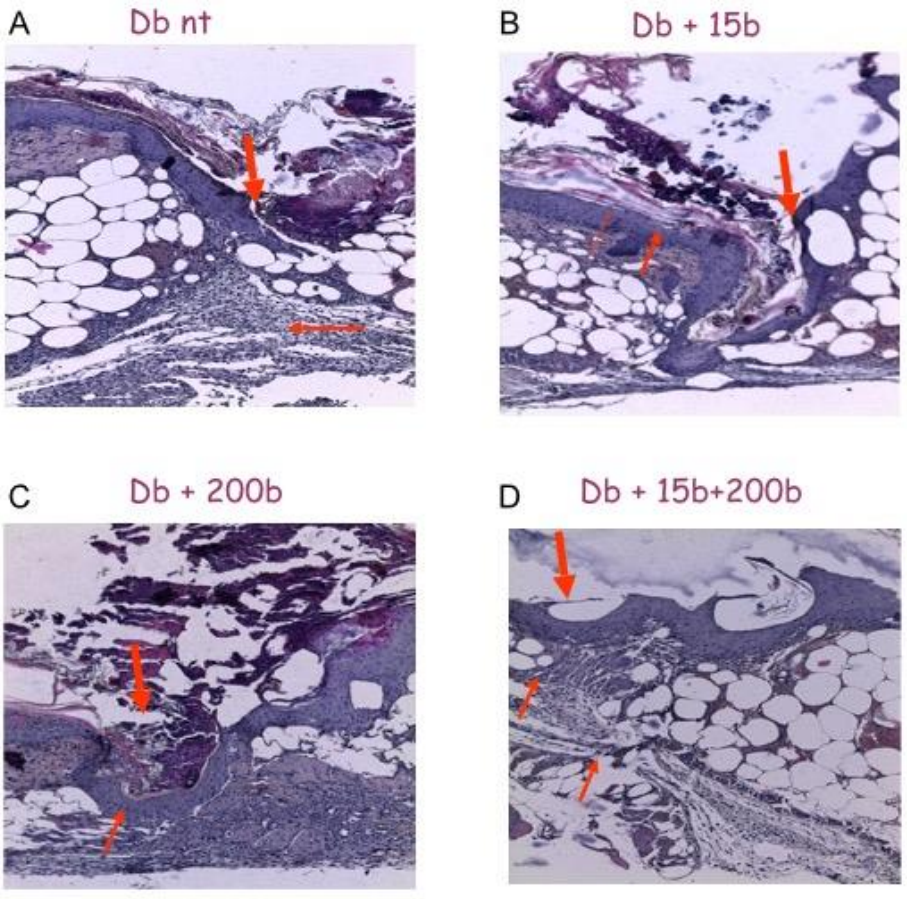

Figure 12

CD31 immunostaining

CD-31 immunostaining was investigated at day 14 to confirm neo-vessel formation (Fig. 16 E-H). Positive staining was present in the wounds from

from diabetic animals injected with vehicle. Administration of Anti-mir augmented CD-31 immunostaining and the positive staining was mostly localized in small vessels and capillaries.

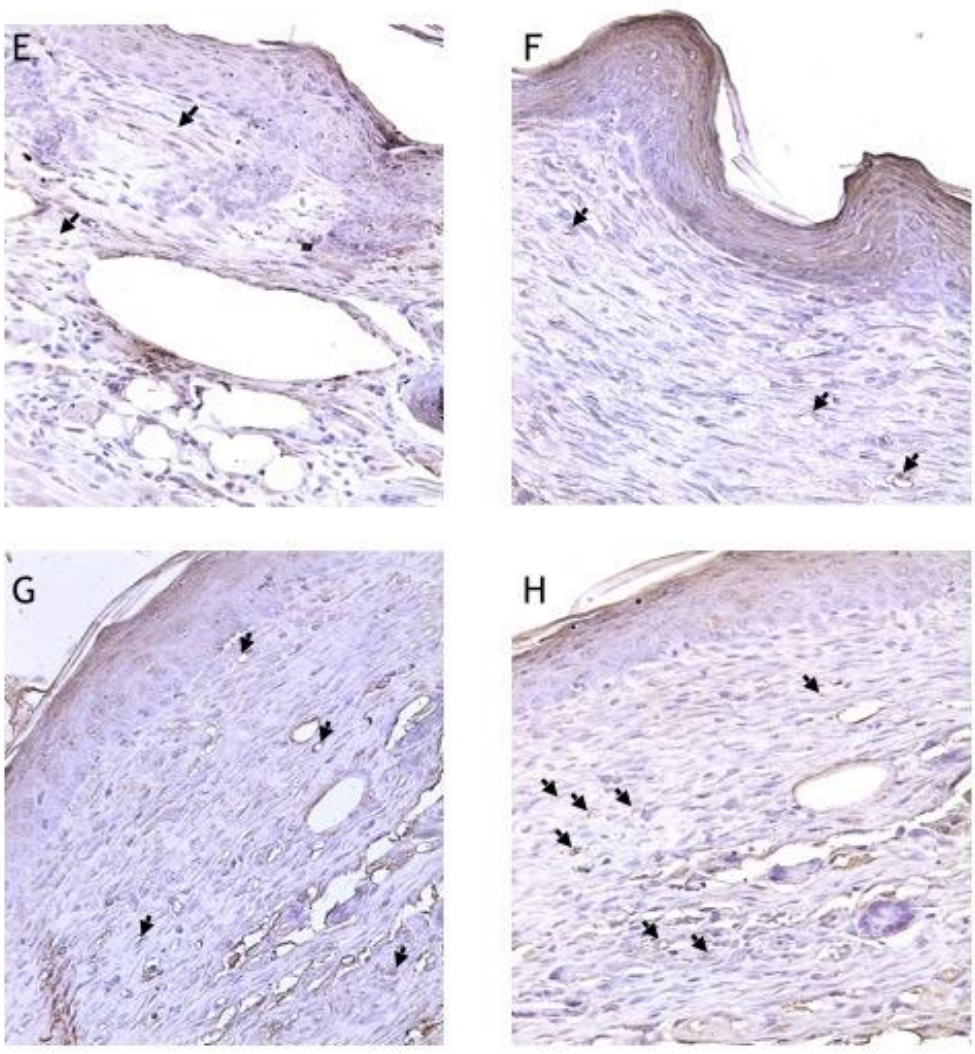

Figure 15

Blood glucose levels and time to wound closure

Wounds are considered closed when the epithelial tissue is completely restored in the area surrounding the incision, and the scab is absent. In

untreated animals, time to wound closure is of 37±2 days after wound productions. Both anti-miR-200b and anti-miR-200b plus anti-miR-15b improved this parameter in a significant manner (Figure 16A-D).

Blood glucose levels were measured at 7 days, right before the sacrifice, to assess if anti-miRs treatment affected the glycaemic values; none of the treatments had an impact on diabetic status of our mice, thus ruling out the hypothesis that our results were due to a general improvement in metabolic features of our experimental animals (Figura 17A).

VEGF expression in liver

To assess if local antagomiRs administration could play a sistemi role, we verified VEGF levels in liver tissue. We did not observed any difference comparing untreated diabetic and healthy animals. Moreover, treatment did not affect the VEGF concentration in liver tissue, thus ruling out the hypothesis of a systemic effect (Figure 17B-C).

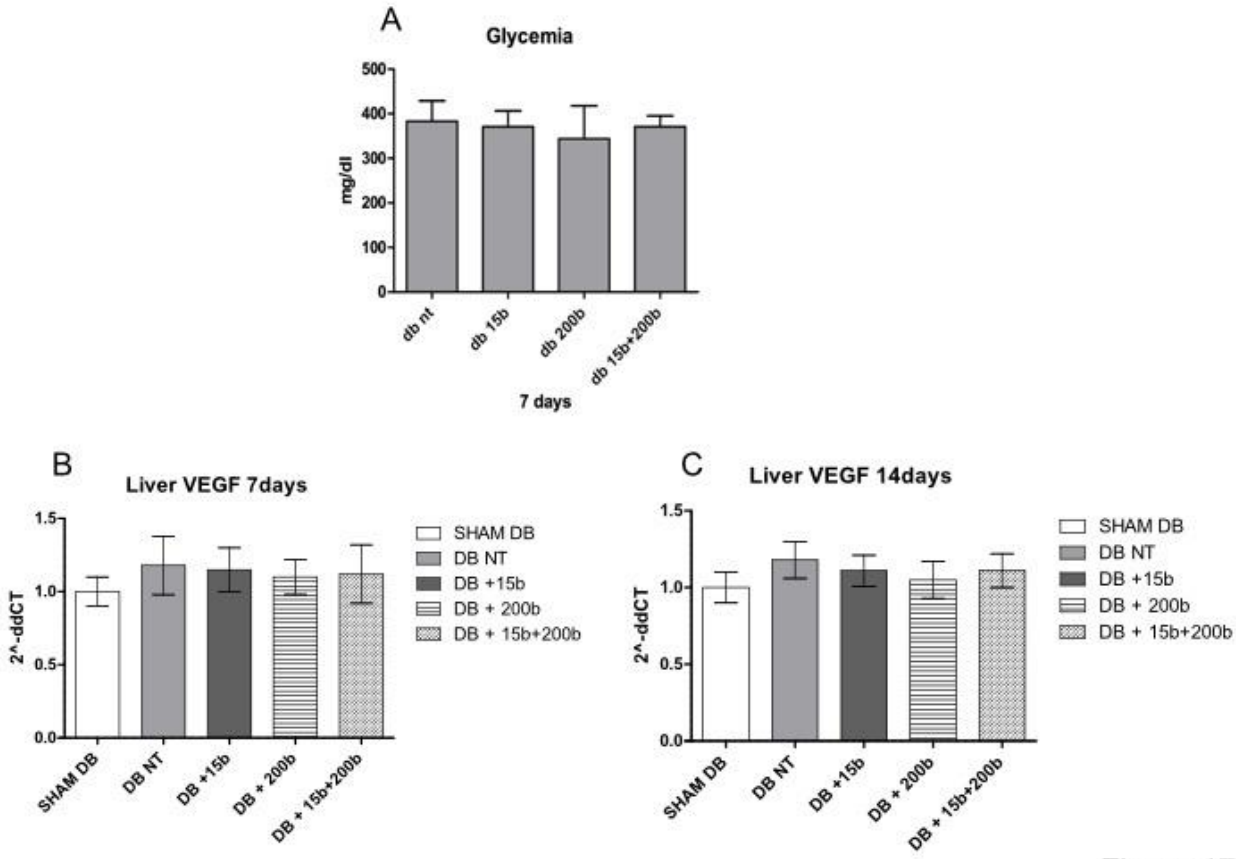
A
Glycemia
mg/dl
500
400
300
200
100
0
db nt
db 15b
db 200b
db 15b+200b
7 days
B
Liver VEGF 7days
2^-ddCT
1.5
1.0
0.5
0.0
SHAM DB
DB NT
DB +15b
DB + 200b
DB + 15b+200b
C
Liver VEGF 14days
2^-ddCT
1.5
1.0
0.5
0.0
SHAM DB
DB NT
DB +15b
DB + 200b
DB + 15b+200b

Figure 17

Discussion

There is a complex cascade of events in skin repair, but angiogenesis is considered a key process during wound healing. A hostile micro-environment in diabetes, mainly due to enhanced production of reactive oxygen species [Altavilla et al., 2001], causes a defect in VEGF-driven angiogenesis that impairs the sequential and coordinated phases of the healing process. The final outcome of skin healing has been suggested to be improved only when the micro-environment is appropriately modified to be favourable for new vessel formation [Galeano et al., 2003; Ishida et al., 2013; Obad et al., 2011; Kong et al., 2010; Unemori et al., 2000; Mookerjee et al., 2005].

Blood vessels form through two distinct processes, vasculogenesis and angiogenesis. In vasculogenesis, endothelial progenitors cells (EPCs) differentiate *de novo* from mesodermal precursors, whereas in angiogenesis new vessels are generated from pre-existing ones. Angiogenesis and neovascularization can be unwanted processes in certain diseases, including cancer. However, formation of the new blood vessels can also help alleviate some states, as in the formation of collateral circulation in ischemic myocardium, limbs as well as during the healing of wounds. There is also in diabetes a well documented disturbance of the mechanisms underlying

vasculogenesis including altered SDF-1α expression, blunted eNOS-NO cascade and reduced EPC mobilization and homing [Brem et al., 2007].

The present findings suggest that a combined stimulation of both angiogenesis and vasculogenesis might represent a rational approach for the management of diabetes-induced impairment, in wound healing, and justify the search of compounds able to afford this task. In this regard the polypeptide hormone relaxin may be of interest. Relaxin has a relevant effect on peripheral and coronary vasculature [Beiler et al., 1960], promotes growth of blood vessels [Stewart, 2009] and induces angiogenesis at wound sites [Ishida et al., 2013].

In our experiment relaxin improved the altered healing process, augmented new vessel formation and increased wound breaking strength in obese-diabetic animals. Relaxin also ameliorated the disturbed pattern of VEGF expression. Interestingly, relaxin stimulated also the expression of CD31, CD34 and VEGFR-1 in new vessels close to the wound site in genetically obese-diabetic mice. In diabetes, the need of neovascularization arises from the inadequate VEGF production and release in wounds: thus, the classic angiogenetic process is extremely delayed and poor and, as a consequence, therapeutically valuable approaches have been addressed to the aim of stimulating the expression of the impaired angiopoietic factor. Our results clearly suggest that relaxin efficiently induces active angiogenesis, in turn

improving the disturbed healing process. However vasculogenesis is also impaired in diabetes and may concur to the reduced pattern of new vessel formation [Brem et al., 2007].

EPCs present the surface marker VEGFR-2 (or *flk-1*) specific for the committed as well as for the young endothelial cells and, driven by growth factors, migrate from the lateral plate mesoderm toward the dorsal aorta to the site of neovasculogenesis [Asahara et al., 1999]. In addition VE-cadherin, an endothelial-specific cell-cell adhesion protein of the adherence junction complex, may represent an additional marker of vasculogenesis [Galeano et al., 2006]. We found a significantly reduced VEGFR-2 and VE-cadherin expression in the wounds of obese-diabetic animals treated with vehicle, while relaxin administration markedly augmented VEGFR-2 and VE-cadherin staining in the vessels close to the surgical injury. Interestingly, we found SDF-1α expression and eNOS-NO cascade to be low expressed at the wound site in db^{+}/db^{+} mice, relaxin treatment succeeded in reverting this defects. These observations confirm that in the diabetic wound healing there is also a defect in vasculogenesis that might also contribute to impair skin repair. Furthermore the present results led us to hypothesize that relaxin may have the ability to generate new vessel formation by a dual mechanism of action including both angiogenesis and vasculogenesis. These effects might represent the main mechanisms by which relaxin ameliorate the skin repair

process. To confirm this hypothesis, we evaluated the time to complete wound closure that represents the “main outcome” for any therapeutic intervention aimed at improving the depressed wound healing in diabetes. Relaxin markedly reduced the time needed to complete skin normalization. Interestingly, the concomitant administration of neutralizing anti-VEGF [Galeano et al., 2011] and SDF-1α receptor CXCR4 antibodies [Galeano et al., 2001] (to interrupt the signalling events involved in the recruitment and homing of EPCs into the ischemic tissue) abated relaxin effects on wound closure, thus confirming our hypothesis. Taking together the immunohistochemical observation and the neutralization experiment demonstrate that relaxin acts through both these pathways to promote angiogenesis and vasculogenesis.

However, a well coordinated healing process does not have to generate an excessive fibrosis that may concur to “disorders” in the skin repair process such as hypertrophic wounds and finally scar formation. Relaxin has been suggested to be therapeutically useful for regulating excessive collagen deposition and promoting tissue remodelling in diseases characterized by fibrotic deposit [Bitto et al., 2013; Bitto et al., 2014]. The mechanism underlying the anti-fibrotic action of relaxin is still far from being fully understood; however the polypeptide hormone has been shown to reduce the activity of some pro-fibrotic factors (i.e. Transforming Growth Factor-ß1

and Interleukin-1ß) [Bani, 2008; Unemori et al., 1999] and to cause metalloproteinases production in some tissue [Piccin et al., 1999]. In agreement with this previous observation, we found that relaxin treatment markedly augmented the staining of MMP-11 in the wounds. This may represent a further positive feature of relaxin treatment, that may well balance collagen turnover, thus avoiding the uncontrolled fibrosis seen in the hypertrophic healing. The relaxin beneficial effect on the disturbed diabetic wound healing was also accompanied by a reduction in blood glucose levels. This effect might be of benefit in the overall management of the diabetic patients, even if it is unlikely that this significant, but "not yet clinically relevant" reduction in blood glucose might contribute to the ralaxin-induced improvement in skin repair.

In conclusion, results from this first experimental study demonstrate that relaxin administration can ameliorate the altered diabetic wound healing not only by accelerating new vessel formation through a "double" mechanism of action, but also by regulating MMP expression, thus avoiding an unwanted and exasperated fibrosis. Since a recombinant form of human relaxin has been studied in Phase II/III clinical trials and demonstrated promising results, particularly in the treatment of acute heart failure [Masini et al., 2004], that is more likely to occur in diabetic patients [Vestweber et al., 2009; Boswell et al., 2011] we believe that our study might shed light on the

possible use of relaxin in diabetic patients with peripheral diseases and local circulatory insufficiency like foot ulcers.

In light of these findings, we considered to exploit further the potential of neoangiogenesis stimulation as strategy to improve wound healing in a diabetic setting. As we discussed before, VEGF is one of the most important mediators of angiogenesis; it is present in high concentration into the area surrounding the lesion, and it is produced by a pletora of cell types, such as keratinocytes, macrophages, and fibroblasts. Several studies in vivo showed that wound healing process may be accelerated and improved when VEGF production is increased. On the other hand, when VEGF is down-expressed, wound healing is impaired and it requires a longer period of time to completely restore tissue. Recently, new molecular mechanisms involved in impaired angiogenesis in diabetic patients have been discovered; in fact, an increase in specific microRNAs seems to affect the physiopathological features of diabetes [Leeper et al., 2011]. MiR-15b e miR-200b are negative modulators in angiogenesis, inhibiting VEGF and VEGFR2 mRNAs processing; in fact, both these miRNAs have been showed to be up-regulated in ulcerated tissue from diabetic mice [Chan et al., 2012; Xu et al., 2014]. These observations lead us to consider an antogomiR-based miR-15b and miR-200b targeting as therapeutic approach to restore the angiogenetic process in diabetic mice.

In our experiments, anti-miR-15b and anti-miR-200b treatment improved the healing process, increasing the amount of new blood vessels in perilesional tissue, recovering at least in part the impaired VEGF pathway. AntagomiRs treatment determined also an increase in TG2, needed to bind VEGF to the ECM and trigger the VEGF-VEGFR2 signaling pathway. In turn, this mehanism lead to an increase in VEGF production iteself, acting as positive feedback-loop, as showed by our results in western blot analysis. At 7 days, we observed also a down-regulation in angiopoietin-1, in all our treatment regimens; this could be due to the fact that angiopoietin-1 decrease during the elargii stage of angiogenesis, thus destabilizing the vessels so that the endothelial cells become able to start sprouting. Treatment with anti-miR-200b, also when combined with anti-miR-15b, was responsible also for the progression in cell cycle, increasing cyclin D1 in nucleus and decreasing the one in cytoplasm; this happens during the G1 phase, while in S phase the opposite is true. From our data seems that anti-miR-200b, alone or combined with anti-miR-15b, had a better effect, probably because increasing the VEGFR2 expression the angiogenic signal is activated in a strongest way.

Gene expression data showed that our antagomiRs together determined an increase in VEGF mRNA levels, as well as that one of Tek, the angiotensin-1 receptor. It is worth to note that, even if mRNA levels are not affected by antagomiRs, protein production can increase as result of a reduction in

miRNA-mediated mRNA degradation. On the other hand, our results did not clarified if antagomiRs can increase also mRNA production, considering that we observed an increase in protein levels not always matched by those of mRNA codifying for that protein.

Angiogenesis stimulation could also represent a negative event in tissues such as retina, liver, and brain. This is true, in example, for those drug that act stimulating angiogenesis in diabetic patients, presenting side effects derived from new vessels formation in tissues that did not requires it. Additionally, angiogenesis stimulation can also have an impact in precancerous states and undetected cancer diseases. In light of these considerations, we assessed the impact of our treatments in liver tissue VEGF expression at 7 days; we did not observed any effect in such tissue, so ruling out the hypothesis that antagomiRs, at least in our experimental conditions, can exert systemic un-desired effects.

The data generated in this second batch of experiments let us to affirm that antagomiRs seem to have an interesting profile in terms of both efficacy and safety, in their *LNA™-enhanced* form. Their local effects seems to be also long lasting, considering we administered the molecule just one time in our esperimental setting. Nonetheless, further studies need to be performed, to fully elucidate the very exact mechanism of action of this antagomiRs, as

well as their viability as potential therapeutic options in pathological conditions involving angiogenesis impairment.

References

Altavilla, D., Saitta, A., Cucinotta, D., Galeano, M., Deodato, B., Colonna, M., Torre, V., Russo, G., Sardella, A., Urna, G., Campo, G.M., Cavallari, V., Squadrito, G. and Squadrito F. (2001) Inhibition of lipid peroxidation restores impaired vascular endothelial growth factor expression and stimulates wound healing and angiogenesis in the genetically diabetic mouse. Diabetes 50, 667-674

Altavilla, D., Squadrito, F., Polito, F., Irrera, N., Calò, M., Lo Cascio, P., Galeano, M., La Cava, L., Minutoli, L., Marini, H. and Bitto, A. (2011) Activation of adenosine A2A receptors restores the altered cell-cycle machinery during impaired wound healing in genetically diabetic mice. Surgery 149, 253-261

Asahara, T., Masuda, H. and Takahashi, T. (1999) Bone marrow origin of endothelial progenitor cells responsible for postnatal vasculogenesis in physiological and pathological neovascularization. Circ. Res. 85, 221-228

Bani, D. (2008) Relaxin as a natural agent for vascular health. Vasc. Health Risk Manag. 4, 515-524

Beiler, J.M., McBurney, E.A., Patchman, E.A., Pizzaia, L.M. and Martin, G.J. (1960) Effects of relaxin on wound healing. Arch. Int. Pharmacodyn. Ther. 123, 291-294

Bitto A, Altavilla D, Pizzino G, Irrera N, Pallio G, Colonna MR, Squadrito F. Inhibition of inflammasome activation improves the impaired pattern of healing in genetically diabetic mice. (2014) Br J Pharmacol. May;171(9):2300-7.

Bitto A, Irrera N, Minutoli L, Calò M, Lo Cascio P, Caccia P, Pizzino G, Pallio G, Micali A, Vaccaro M, Saitta A, Squadrito F, Altavilla D. Relaxin improves multiple markers of wound healing and ameliorates the disturbed healing pattern of genetically diabetic mice. (2013) Clin Sci (Lond). Dec;125(12):575-85.

Boswell, C.A., Ferl, G.Z., Mundo, E.E., Bumbaca, D., Schweiger, M.G., Theil, F.P., Fielder, P.J. and Khawli, L.A. (2011) Effects of anti-VEGF on predicted antibody biodistribution: roles of vascular volume, interstitial volume, and blood flow. PLoS One 6, e17874

Brem, H. and Tomic-Canic, M. (2007) Cellular and molecular basis of wound healing in diabetes. J. Clin. Invest. 117, 1219-1222

Chan YC, Roy S, Khanna S, Sen CK. Downregulation of endothelial microRNA-200b supports cutaneous wound angiogenesis by desilencing GATA binding protein 2 and vascular endothelial growth factor receptor 2. (2012) Arterioscler Thromb Vasc Biol. Jun;32(6):1372-82.

Falanga, V. (2005) Wound healing and its impairment in the diabetic foot. Lancet 366, 1736-1743

Ferrara, N., Gerber, H.P. and LeCouter, J. (2003) The biology of VEGF and its receptors. Nat. Med. 9, 669-676

Galeano, M., Altavilla, D., Bitto, A., Minutoli, L., Calò, M., Lo Cascio, P., Polito, F., Giugliano, G., Squadrito, G., Mioni, C., Giuliani, D., Venuti, F.S. and Squadrito, F. (2006) Recombinant human erythropoietin improves angiogenesis and wound healing in experimental burn wounds. Crit. Care Med. 34, 1139-1146.

Galeano, M., Bitto, A., Altavilla, D., Minutoli, L., Polito, F., Calò, M., Lo Cascio, P., Stagno d'Alcontres, F. and Squadrito, F. (2008) Polydeoxyribonucleotide stimulates angiogenesis and wound healing in the genetically diabetic mouse. Wound Repair. Regen. 16, 208-217

Galeano, M., Deodato, B., Altavilla, D., Cucinotta, D., Arsic, N., Marini, H., Torre, V., Giacca, M. and Squadrito F. (2003) Adeno-associated viral vector-mediated human vascular endothelial growth factor gene transfer stimulates angiogenesis and wound healing in the genetically diabetic mouse. Diabetologia 46, 546-555

Galeano, M., Polito, F., Bitto, A., Irrera, N., Campo, G.M., Avenoso, A., Calò, M., Lo Cascio, P., Minutoli, L., Barone, M., Squadrito, F. and Altavilla, D. (2011) Systemic administration of high-molecular weight hyaluronan stimulates wound healing in genetically diabetic mice. Biochim. Biophys. Acta 18127:752-759

Galeano, M., Torre, V., Deodato, B., Campo, G.M., Colonna, M., Sturiale, A., Squadrito, F., Cavallari, V., Cucinotta, D., Buemi, M. and Altavilla, D. (2001) Raxofelast, a hydrophilic vitamin E-like antioxidant, stimulates wound healing in genetically diabetic mice. Surgery 129, 467-477

Ishida M, Selaru FM. miRNA-Based Therapeutic Strategies. (2013) Curr Anesthesiol Rep. Mar 1;1(1):63-70.

Kilkenny C, Browne WJ, Cuthill IC, Emerson M, Altman DG. Improving bioscience research reporting: The ARRIVE guidelines for reporting animal research. (2010) J Pharmacol Pharmacother. Jul;1(2):94-9.

Kong, R.C., Shilling, P.J., Lobb, D.K., Gooley, P.R. and Bathgate, R.A. (2010) Membrane receptors: structure and function of the relaxin family peptide receptors. Mol. Cell Endocrinol. 320, 1-15

Laganà A, Shasha D, Croce CM. Synthetic RNAs for Gene Regulation: Design Principles and Computational Tools. (2014) Front Bioeng Biotechnol. Dec 11;2:65.

Leeper NJ, Cooke JP. MicroRNA and mechanisms of impaired angiogenesis in diabetes mellitus. (2011) Circulation. Jan 25;123(3):236-8.

Masini, E., Nistri, S., Vannacci, A., Bani Sacchi, T., Novelli, A. and Bani, D. (2004) Relaxin inhibits the activation of human neutrophils: involvement of the nitric oxide pathway. Endocrinology 145, 1106-1112

Mookerjee, I., Unemori, E.N., Du, X.J., Tregear, G.W. and Samuel, C.S. (2005) Relaxin modulates fibroblast function, collagen production, and matrix metalloproteinase-2 expression by cardiac fibroblasts. Ann. N. Y. Acad. Sci. 1041, 190-193

Obad S, dos Santos CO, Petri A, Heidenblad M, Broom O, Ruse C, Fu C, Lindow M, Stenvang J, Straarup EM, Hansen HF, Koch T, Pappin D, Hannon GJ, Kauppinen S. Silencing of microRNA families by seed-targeting tiny LNAs. Nat Genet. 2011;43(4):371–378

Peichev, M., Naiyer, A.J., Pereira, D., Zhu, Z., Lane, W.J., Williams, M., Oz, M.C., Hicklin, D.J., Witte, L., Moore, M.A. and Rafii, S. (2000) Expression of VEGFR-2 and AC133 by circulating human CD34+ cells identifies a population of functional endothelial precursors. Blood 95, 952-958

Peplow PV, Baxter GD. Gene expression and release of growth factors during delayed wound healing: a review of studies in diabetic animals and possible combined laser phototherapy and growth factor treatment to enhance healing. (2012) Photomed Laser Surg. Nov;30(11):617-36.

Piccinni, M.P., Bani, D., Beloni, L., Manuelli, C., Mavilia, C., Vocioni, F., Bigazzi, M., Sacchi, T.B., Romagnani, S. and Maggi, E. (1999) Relaxin favors the development of activated human T cells into Th1-like effectors. Eur. J. Immunol. 29, 2241-2247

Reiber, G.E. and Raugi, G.J. (2005) Preventing foot ulcers and amputations in diabetes. Lancet 366, 1676-1677

Singh, N., Armstrong, D.G. and Lipsky, B.A. (2005) Preventing foot ulcers in patients with diabetes. JAMA 293, 217-228

Stewart, D.R. (2009) Scar prevention and cosmetically enhanced wound healing usingrelaxin. Ann. N. Y. Acad. Sci. 1160, 336-341

Tammela, T., Enholm, B., Alitalo, K. and Paavonen, K. (2005) The biology of vascular endothelial growth factors. Cardiovasc. Res. 65, 550-563

Unemori, E.N. and Amento, E.P. (1990) Relaxin modulates synthesis and secretion of procollagenase and collagen by human dermal fibroblasts. J. Biol. Chem. 265, 10681-10685

Unemori, E.N., Erikson, M.E., Rocco, S.E., Sutherland, K.M., Parsell, D.A., Mak, J. and Grove, B.H. (1999) Relaxin stimulates expression of vascular endothelial growth factor in normal human endometrial cells in vitro and is associated with menometrorrhagia in women. Hum. Reprod. 14, 800-806

Unemori, E.N., Lewis, M., Constant, J., Arnold, G., Grove, B.H., Normand, J., Deshpande, U., Salles, A., Pickford, L.B., Erikson, M.E., Hunt, T.K. and Huang, X. (2000) Relaxin induces vascular endothelial growth factor expression and angiogenesis selectively at wound sites. Wound Repair. Regen. 8, 361-370

Urbich, C. and Dimmeler, S. (2004) Endothelial progenitor cells functional characterization. Trends Cardiovasc. Med. 14, 318-322.

Vestweber, D., Winderlich, M., Cagna, G. and Nottebaum, A.F. (2009) Cell adhesion dynamics at endothelial junctions: VE-cadherin as a major player. Trends Cell Biol. 19, 8-15

Wetzler, C., Kampfer, H., Stallmeyer, B., Pfeilschifter, J. and Frank, S. (2000) Large and sustained induction of chemokines during impaired wound healing in the genetically diabetic mouse: prolonged persistence of neutrophils and macrophages during the late phase of repair. J. Invest. Dermatol. 115, 245-253

Xu J, Zgheib C, Hu J, Wu W, Zhang L, Liechty KW. The role of microRNA-15b in the impaired angiogenesis in diabetic wounds. (2014) Wound Repair Regen. Sep-Oct;22(5):671-7.

Figure legend

Figure 1.

A: The cartoon represents the back of a mice with the site of the two wounds and of the implanted pump; on the right side is represented an excised wound (ellipse shaped) that is subdivided in pieces to perform all the analysis. The breaking strength analysis is performed on an entire wound, following excision. At the bottom the timeline of the experiment is represented.

B: VEGF mRNA expression in skin wound samples collected from normoglycaemic ($db^{+/+}m$) mice treated with different RLX doses (6.25, 12.5, 25 and 50µg/mouse/day) at day 6. Each bar represents the mean ± S.D. of six animals. *$p<0.05$ vs RLX 6.25; $^{\#}p<0.001$ vs RLX 6.25.

VEGF (**C**) and SDF1-α (**E**) mRNA expression in skin wound samples collected from either normoglycaemic ($db^{+/+}m$) and diabetic mice (db^{+}/db^{+}) given either RLX (25µg/mouse/day/s.c.) or vehicle (6µl/mouse/day of 0.9 % NaCl) at 3, 6 and 12 days. Each point represents the mean ± S.D. of six animals. $^{\S}p<0.001$ vs $db^{+/+}m$ + vehicle; *$p<0.05$ vs $db^{+/+}m$ + vehicle; $^{\#}p<0.001$ vs db^{+}/db^{+} + vehicle.

D: VEGF protein levels studied by ELISA in skin wound samples collected from either normoglycaemic ($db^{+/+}m$) and diabetic mice (db^{+}/db^{+}) given either RLX (25µg/mouse/day/s.c.) or vehicle (6µl/mouse/day of 0.9 % NaCl) at 3, 6 and 12 days. Each point represents the mean ± S.D. of six animals. $^{\S}p<0.001$ vs $db^{+/+}m$ + vehicle; *$p<0.05$ vs $db^{+/+}m$ + vehicle; $^{\#}p<0.001$ vs db^{+}/db^{+} + vehicle.

Figure 2

eNOS expression (constitutive and phosphorilated form) (**A**) and NO products (**B**) in skin wound samples collected from either normoglycaemic ($db^{+/+}m$) and diabetic mice (db^{+}/db^{+}) given either RLX

(25µg/mouse/day/s.c.) or vehicle (6µl/mouse/day of 0.9 % NaCl) at day 6. Each bar represents the mean ± S.D. of six animals. *$p<0.01$ vs $db^{+/+}m$ + vehicle; §$p<0.05$ vs $db^{+/+}m$ + vehicle; #$p<0.05$ vs db^{+}/db^{+} + vehicle.

Figure 3

A: Histological scores in wound samples collected from either normoglycaemic ($db^{+/+}m$) and diabetic mice (db^{+}/db^{+}) given either RLX (25µg/mouse/day/s.c.) or vehicle (6µl/mouse/day of 0.9 % NaCl) at day 12. Each bar represents the mean ± S.D. of six animals. §$p<0.001$ vs $db^{+/+}m$ + vehicle; #$p<0.001$ vs db^{+}/db^{+} + vehicle.

B, C, D and E: Histological photomicrographs, haematoxylin-eosin, of the several experimental groups at day 12.

B: Vehicle treated normoglycaemic ($db^{+/+}m$) wounds. Re-epithelialization is almost complete. Granulation tissue is well-formed without inflammatory infiltrates.

C: RLX treated normoglycaemic ($db^{+/+}m$) wounds. Complete re-epithelialization and restoration of normal architecture in dermis.

D: Vehicle treated diabetic (db^{+}/db^{+}) wounds. Incomplete re-epithelialization and poorly-formed granulation tissue.

E: RLX treated diabetic (db^{+}/db^{+}) wounds. Re-epithelialization is almost complete, well-organized granulation tissue and no evidence of inflammation, oedema or erythrorrhagies.

Figure 4.

Time to complete the wound closure in normoglycaemic ($db^{+/+}m$) and diabetic mice (db^{+}/db^{+}) given either RLX (25µg/mouse/day/s.c.) or vehicle (6µl/mouse/day of 0.9 % NaCl). Two additional grups of diabetic animals were administered with RLX (25µg/mouse/day/s.c.) and treated with an anti-

VEGF murine antibody (10mg/kg/i.p. daily) or with anti CXCR4 antibody (0.4 mg/kg/i.p. daily). Each point represents the mean ± S.D. of six animals. $^{§}p<0.001$ vs $db^{+/+}m$ + vehicle or relaxin; $*p<0.05$ vs $db^{+/+}m$ + vehicle; $^{\#}p<0.001$ vs db^{+}/db^{+} + vehicle; $^{\circ}p<0.05$ vs db^{+}/db^{+} + RLX.

Figure 5.

A and B: Representative immunohistochemical CD31 staining of skin wounds samples from from diabetic (db^{+}/db^{+}) mice given with vehicle (6µl/mouse/day of 0.9 % NaCl) or RLX (25µg/mouse/day s.c.) at day 12. Arrows indicate staining positivity.

C: Comparison of semiquantitative assessment of microvascular density (MVD) between each group. Each bar represents the mean ± S.D. of six animals. $*p<0.05$ vs $db^{+/+}m$ + vehicle; $^{§}p<0.01$ vs $db^{+/+}m$ + vehicle; $^{\#}p<0.01$ vs db^{+}/db^{+} + vehicle.

Figure 6.

A and B: Representative immunohistochemical CD34 staining of skin wound samples from diabetic (db^{+}/db^{+}) mice given with vehicle (6µl/mouse/day of 0.9 % NaCl) or RLX (25µg/mouse/day/s.c.) at day 12. Arrows indicate staining positivity.

C **and D:** Representative immunohistochemical VEGFR-1 staining of skin wound samples from diabetic (db^{+}/db^{+}) mice given with vehicle (6µl/mouse/day of 0.9% NaCl) or RLX (25µg/mouse/day/s.c.) at day 12. Arrows indicate staining positivity.

E **and F:** Quantification of CD34 (E) and VEGF-R1 (F) positive cells per field in normoglycaemic ($db^{+/+}m$) and diabetic (db^{+}/db^{+}) mice given with vehicle (6µl/mouse/day of 0.9% NaCl) or with RLX (25µg/mouse/day/s.c.)

at day 12. Each bar represents the mean ± S.D. of six animals. *p<0.05 vs $db^{+/+}m$ + vehicle; §p<0.01 vs $db^{+/+}m$ + vehicle; #p<0.01 vs db^{+}/db^{+} + vehicle.

Figure 7.

A and B: Representative immunohistochemical VEGFR-2 staining of skin wounds samples from diabetic (db^{+}/db^{+}) mice given with vehicle (6µl/mouse/day of 0.9 % NaCl) or RLX (25µg/mouse/day/s.c.) at day 12. Arrows indicate staining positivity.

C and D: Representative immunohistochemical VE-cadherin staining of skin wounds samples from diabetic (db^{+}/db^{+}) mice given with vehicle (6µl/mouse/day of 0.9 % NaCl) or RLX (25µg/mouse/day/s.c.) at day 12. Arrows indicate staining positivity.

E and F: Quantification of VEGF-R2 and VE-Cadherin positive cells per field in normoglycaemic ($db^{+/+}m$) and diabetic (db^{+}/db^{+}) mice given with vehicle (6µl/mouse/day of 0.9 % NaCl) or with RLX (25µg/mouse/day/s.c.) at day 12. Each bar represents the mean ± S.D. of six animals. *p<0.05 vs $db^{+/+}m$ + vehicle; §p<0.01 vs $db^{+/+}m$ + vehicle; #p<0.01 vs db^{+}/db^{+} + vehicle.

Figure 8.

A and B: Representative immunohistochemical MMP-11 staining of skin wound samples from diabetic (db^{+}/db^{+}) mice given with vehicle (6µl/mouse/day of 0.9% NaCl) or RLX (25µg/mouse/day/s.c.) at day 12. Arrows indicate staining positivity.

C: Quantification of MMP-11 staining per field in normoglycaemic ($db^{+/+}m$) and diabetic (db^{+}/db^{+}) mice given with vehicle (6µl/mouse/day of 0.9 % NaCl) or with RLX (25µg/mouse/day/s.c.) at day 12. Each bar represents the

mean ± S.D. of six animals. *$p<0.05$ vs $db^{+/+}m$ + vehicle; $^{\#}p<0.01$ vs db^{+}/db^{+} + vehicle.

Figure 9.

Tensile strength of wounds (**A**) and blood glucose levels (**B)** obtained at day 12 from normoglycaemic ($db^{+/+}m$) and diabetic mice (db^{+}/db^{+}) administered with either RLX (25µg/mouse/day/s.c.) or vehicle (6µl/mouse/day of 0.9% NaCl). Each bar represents the mean ± S.D. of six animals. $^{\S}p<0.01$ vs $db^{+/+}m$ + vehicle; $^{\#}p<0.05$ vs db^{+}/db^{+} + vehicle.

Figure 10.

VEGF mRNA expression in skin tissue, quantified by RT-qPCR at both 7 (**A**) and 14 days (**B**) after surgical procedures.

Figure 11.

AGPT mRNA expression in skin tissue, quantified by RT-qPCR at both 7 (**A**) and 14 days (**B**) after surgical procedures, and TEK mRNA expression, obtained at the very same time points (7 days, **C**; 14 days, **D**).

Figure 12.

Hematoxilyn-Eosin staining of perilesional skin tissue from diabetic animals untreated (**A**), o treated with anti-15b (**B**), anti-200b (**C**), and anti-15b+200b (**D**), 7 days after surgical procedures. Red arrows are used to mark wound incisions.

Figure 13.

VEGF protein assessment was performed by western blot from skin tissue; animal receiving anti-15b (**A**), anti-200b (**B**), and anti-15b+200b (**C**) showed

a statistically significant increase in VEGF protein compared to untreated animals. VEGFR2 protein was detected performing immunohistochemistry (Fig. 13 **D**, **E**, **F**, and **G**).

Figure 14.

Transglutaminase-2 protein quantification by western blot from skin tissue; anti-15b (**A**), anti-200b (**B**), determined a statistically significant increase in protein compared to untreated animals; anti-15b+200b (**C**) administration was responsible for a trend in increase of TG2 protein, not in a significant manner. Masson's trichrome was used to highlight sub-epithelial connective tissue restoration, with or without antagomirs administration (Fig. 14 **D**, **E**, **F**, and **G**).

Figure 15.

Hematoxilyn-Eosin staining of perilesional skin tissue from diabetic animals untreated (**A**), o treated with anti-15b (**B**), anti-200b (**C**), and anti-15b+200b (**D**), 14 days after surgical procedures. CD31 staining was performed to assess new vessels formation, which is increased in animals treated (anti-15b, **F**; anti-200b, **G**; anti-15b+200b, **H**) compared to controls (**E**)

Figure 16.

Time to complete healing (**A**) was assessed, in order to verify if treatments were able to significantly improve this parameter. Panels **B**, **C**, and **D** show the macroscopic appearance of a rapresentative animal for each treatment group at the time of wound closure. Panel **E** shows the values obtained by tensile strenght analysis.

Figure 17.

Panel **A** shows glycemic values for each group of animals 7 days after surgery, in order to verify that our experimental findings were not affected by a remission of hyper-glycemia. Panels **B** and **C** show VEGF mRNA expression in liver, 7 days (**B**) and 14 days (**C**) after surgery, to exclude systemic effects of our treatme